AAO2 impairment improves aldehyde detoxification by AAO3 in Arabidopsis leaves exposed to UVC or Rose Bengal.

Zhadyrassyn Nurbekova[a], Sudhakar Srivastava[a], Nja Zai Du[b], Veronica Turečková[c], Miroslav Strand[c], Rustem Omarov[d], Moshe Sagi[e,f]*

[a]Jacob Blaustein Center for Scientific Cooperation, The Jacob Blaustein Institutes for Desert Research, Ben-Gurion University of the Negev, Sede Boqer Campus, 8499000, Israel.

[b]The Albert Katz International School for Desert Studies, The Jacob Blaustein Institutes for Desert Research, Ben-Gurion University of the Negev, Sede Boqer Campus, 8499000, Israel

[c]Laboratory of Growth Regulators, The Czech Academy of Sciences, Institute of Experimental Botany, Palacky University, Slechtitelu 27, CZ-78371, Olomouc, Czech Republic

[d]Department of Biotechnology and Microbiology, L.N. Gumilyov Eurasian University, Astana, Kazakhstan

[e]The Albert Katz Department of Dryland Biotechnologies, French Associates Institute for Agriculture and Biotechnology of Dryland, The Jacob Blaustein Institutes for Desert Research, Ben-Gurion University of the Negev, Sede Boqer Campus, 8499000, Israel.

[f]Katif Research Center for Development of Coastal Deserts, Netivot 87710, Israel.

*Address correspondence to gizi@bgu.ac.il

The author responsible for distribution of materials integral to the findings presented in this article in accordance with the policy described in the Instructions for Authors (https://academic.oup.com/plphys/pages/General-Instructions) is: Moshe Sagi (gizi@bgu.ac.il).

Short running head: **AAO2 mutation induces AAO3 activity.**

Abstract

Among the three active aldehyde oxidases in *Arabidopsis thaliana* leaves (AAO1-3), AAO3, which catalyzes the oxidation of abscisic-aldehyde to abscisic-acid, was shown recently to function as a reactive aldehyde detoxifier. Notably, *aao2KO* mutants exhibited less senescence symptoms and lower aldehyde accumulation, such as acrolein, benzaldehyde, and HNE than in wild-type leaves exposed to UV-C or Rose-Bengal. The effect of the absence of AAO2 expression on aldehyde detoxification by AAO3 and/or AAO1 was studied by comparing the response of wild-type plants to the response of *aao1Single* mutant, *aao2KO* mutants and single mutants of *aao3Ss*. Notably, *aao3Ss* exhibited similar aldehyde accumulation and chlorophyll content to *aao2KO* treated with UV-C or Rose-Bengal. In contrast, wild-type and *aao1S* exhibited higher aldehyde accumulation that resulted in lower

remaining chlorophyll than in aao*2KO* leaves, indicating that the absence of active AAO2 enhanced AAO3 detoxification activity in *aao2KO* mutants. In support of this notion, employing abscisic-aldehyde as a specific substrate marker for AAO3 activity revealed enhanced AAO3 activity in *aao2KO* and *aao3Ss* leaves compared to wild-type treated with UV-C or Rose Bengal. The similar abscisic acid level accumulated in leaves of unstressed or stressed genotypes indicates that aldehyde detoxification by AAO3 is the cause for better stress resistance in *aao2KO* mutants. Employing the sulfuration process (known to activate aldehyde oxidases) in wild-type, *aao2KO*, and *molybdenum-cofactor sulfurase* (*aba3-1*) mutant plants revealed that the active AAO2 in WT employs sulfuration processes essential for AAO3 activity level, resulting in the lower AAO3 activity in WT than AAO3 activity in *aao2KO.*

Keywords: Arabidopsis, aldehyde oxidase, reactive aldehydes, senescence, UV-C irradiation, Rose Bengal, aldehyde toxicity, Sulfuration

Introduction

Aldehyde oxidase (AO) is a cytoplasmic multicomponent domain enzyme which contains FAD, Fe-S and molybdenum cofactor (MoCo) as its prosthetic groups and thus belongs to the family of Mo-hydroxylases (Koshiba et al. 1996; Yesbergenova et al. 2005). AO catalyzes the oxidation of a variety of aldehydes and heterocyclic compounds, thereby converting them to the respective carboxylic acids (Koshiba et al. 1996, Akaba et al. 1998; Seo et al. 2000a; Seo et al. 2002; Srivastava et al. 2017). AO enzymes have a relatively broad substrate specificity and their role in response to environmental stress factors was previously reported (Omarov et al. 1998; Sagi et al. 1998; Zdunek-Zastocka et al. 2004; Yergaliyev et al. 2016). Early observations demonstrated the presence of four AO genes in *Arabidopsis thaliana* and their organ localization as well as their expression dependency on the developmental stage of the organ. *Arabidopsis* AO1 (AAO1) was shown to be mainly expressed in seeds, roots and seedlings, AAO2 in seedlings and roots, AAO3 in rosettes and roots whereas AAO4 is mainly expressed in siliques (Seo et al. 2000a; Koiwai et al., 2004; Srivastava et al. 2017). Additionally, it was shown that AAO1 is involved in the oxidation of indole-3-carboldehyde (ICHO) to indole-3-carboxylic acid (ICOOH) (Bottcher et al., 2014) and AAO4 is involved in benzoic acid biosynthesis (Ibdah et al. 2009). Additionally, it was demonstrated that AAO4 can efficiently oxidize toxic aldehydes and thus delay silique senescence (Srivastava et al. 2017). Recently it was shown that AAO3 known to oxidize abscisic aldehyde (ABal) to abscisic acid (ABA) (Seo et al. 2000a, 2000b;), can protect rosette leaves from stressed induced

68 aldehyde toxicity (Nurbekova et al. 2021). Additional roles for AAO2 and the other AAOs
69 require further investigation.

70 Plants are constantly exposed to environmental factors such as extreme temperature,
71 drought, salinity, pathogen attack and natural aging which leads to enhanced generation of
72 aldehydes, downstream to reactive oxygen species (ROS) production. Above a certain level,
73 specific to each of the aldehydes, the elevated level of aldehydes can be toxic, leading to the
74 oxidative injury of plants, enhanced chlorophyll degradation, hastened senescence, and even
75 cell death (Biswas and Mano, 2016; Srivastava et al. 2017; Nurbekova et al. 2021).
76 Detoxification of the increased aldehydes is therefore essential for plant survival and was
77 shown by aldehyde dehydrogenases [ALDH; EC 1.2.1.3 (Sunkar et al. 2003; Stiti et al. 2011;
78 Widhalm and Dudareva, 2015)], aldo-keto reductases (AKR; EC 1.1.1.2), aldehyde reductases
79 [ALR; EC 1.1.1.2 (Oberschall et al. 2000; Yamauchi et al. 2011)], 2-alkenal reductases [AER,
80 EC 1.3.1.74 (Mano et al. 2002)], glutathione transferase tau isozymes [GST (Mano et al.
81 2019)], and aldehyde oxidases 3 and 4 (Srivastava et al. 2017; Nurbekova et al. 2021).

82 Recently we observed a significant reduction of AAO2 in-gel activity in plants exposed
83 to UV-C irradiation [Nurbekova et al. 2021; (Fig.7J)], which led us to investigate a possible
84 role of AAO2 in plants exposed to abiotic stresses. In the current study better detoxification of
85 aldehydes in the *aldehyde oxidase 2* knock out (*aao2 KO*) mutants than in WT in response to
86 UV-C irradiation or Rose Bengal application was shown. The application of such stresses
87 resulted in higher chlorophyll degradation in WT leaves, the result of a better oxidation of these
88 aldehydes by *aao2 KO* mutant than in WT. Since *aao2 KO* mutant leaves contains active AAO1
89 and AAO3, by employing RNA interference (RNAi) on the various T-DNA KO mutants
90 impaired in one of the three aldehyde oxidases AAO1-3, single mutants were generated and
91 were exposed to UV-C irradiation or Rose Bengal application. Notably, independent *aao3*
92 single (*aao3Ss*) mutants containing fully active AAO3 exhibited lower aldehyde accumulation
93 as compared to WT, while *aao1* single (*aao1Ss*) mutants, containing fully active AAO1
94 resulted in similar or higher level of aldehyde accumulation as well as higher chlorophyll
95 degradation as compared to WT under UV-C irradiation or Rose Bengal application, indicating
96 that the impairment of AAO2 causes the enhancement of AAO3 activity and the capacity of
97 carbonyl aldehyde detoxification in Arabidopsis.

98

99 **Results**

Protein expression analysis of *aao2* KO and identification of AAO2 activity

To investigate the possible roles of AAO2 in aldehyde detoxification two independent knock-out (KO) lines of *aao2* mutants [SALK_104895 (KO-95) and SAIL_563_G09 (KO-563)] each carrying exon inserted T-DNA, were employed. The homozygosity of the two *aao2* KO lines were examined. The absence of amplicon when using gene specific left and right primers (LP+RP) and the presence of amplicon with RP and T-DNA specific primers (LB1.3/LB2) indicated the homozygous lines for the knockout mutants of *AAO2* (Fig.1A and Supplemental Table S1). The transcript expression of *AAO2* was determined by quantitative polymerase chain reaction (qPCR) using gene specific primers from either side of T-DNA insertion (Supplemental Tables S2A). No expression was detected in *aao2 KO* mutants, whereas in WT the expression of *AAO2* was evident (Fig.1B) and the amplicons were verified by sequencing (Table *S2B*).

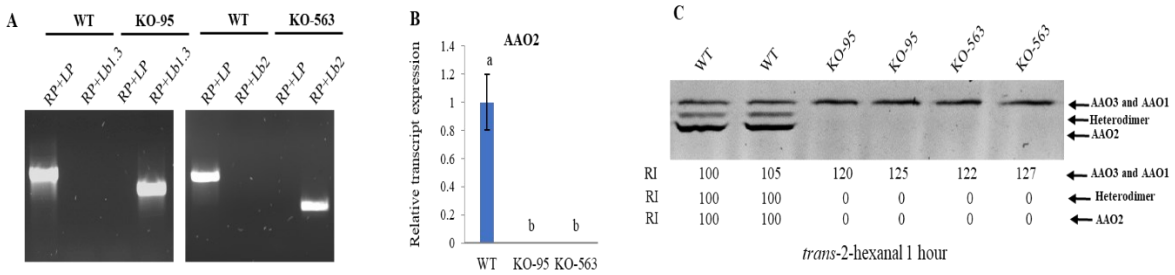

Figure 1. Characterization of *Arabidopsis* aldehyde oxidase 2 mutants. **A.** Verification of AAO2 knock out mutants {*aao2* [SALK_104895 (KO-95) and SAIL_563_G09 (KO-563)]} by PCR using the combination of gene specific primers (LP and RP) and specific primer flanking T-DNA insertion stretches (LB 1.3 or LB2, respectively). **B.** Relative transcript expression of *AAO2* (At3g43600) in WT and the two *aao2* mutants' rosette leaves. The expression of the *AAO2* in each genotype was compared against *AAO2* in WT after normalization to *Arabidopsis EF-1a* (At5g60390) as the housekeeping gene product and presented as the relative expression. Values means ± SE (n=3). Differences were compared among all the genotypes and different letters show the significant difference between genotypes (Tukey's honest significant difference, HSD, P value <0.05). **C.** *Arabidopsis* aldehyde oxidases (AAOs) in-gel activity in WT and *aao2* (KO-95 and KO-563). One hundred µg protein extract from three-week old plants' rosette leaves were fractionated by NATIVE PAGE and AO activity detection with 1 mM *trans*-2-hexanal as the substrate was determined in a reaction solution containing 100 mM Tris-HCl (pH 7.5), 1 mM 3-(4,5-dimethylthiazol-2-yl)-2,5-diphenyltetrazolium bromide and 0.1 mM phenazine methosulfate. The arrow indicates the position of the activity bands generated by AAO1 and AAO3 proteins (uppermost band), middle (heterodimer containing AAO2 with AAO1 and/or with AAO3), and AAO2 (lowermost band). Relative intensity (RI) was estimated by using ImageJ software (https://imagej.nih.gov/ij/) for each activity band. The intensity of the upper, middle, and lowest activity bands in WT was used as reference (100%).

Crude proteins extracted from WT rosette leaves and both *aao2* KOs were employed for the determination of AAO2 in-gel activity by using *trans*-2-hexanal as a substrate (Koshiba et al. 1996; Akaba et al. 1998, 1999; Omarov et al. 1999; Koiwai et al. 2004; Seo et al. 2000a, 2000b; Srivastava et al., 2017). The oxidation of *trans*-2-hexanal led to a highest intensity in the most migrated band and a weaker intensity in the middle band in WT, whereas absence of the middle and the most migrated activity bands was evident in both *aao2* KOs. Notably, the only upper activity band that appeared in *aao2* KOs had a higher band intensity compared to WT (Fig.1C).

120 To further verify that among the aldehyde oxidases only AAO2 generates the most migrated
121 (lowest) activity band, the lowest activity band in *aao1*, *aao3* KOs and WT (Fig.1C) were
122 excised and peptide sequencing was carried out. The sequencing of trypsinized peptides of the
123 lowest activity band of WT, *aao1* and *aao3* KO mutants revealed 8, 6 and 8 unique peptides of
124 AAO2 respectively (Supplemental Table S3). Additionally, AVSGNLCR and IPTVDTIPK
125 were identified in AAO2 activity band of WT, which share identical sequences in AAO1 and
126 AAO3 respectively. VGGGFGGK peptide of AAO2 that was identified in AAO2 activity band
127 in *aao1KO*, shares identical sequences in AAO1 and AAO3. Similarly, the
128 ASGEPPLLLAASVHCATR peptide of AAO2 identified in *aao3,* shares an identical sequence
129 with AAO3 and therefore in all possible likelihood, it belongs to the AAO2 protein activity
130 band.

131 Mutation in AAO2 confers higher capacity of oxidizing aldehydes in *aao2 KO* 132 mutants as compared to WT.

133 The capacity of *aao2* mutant to oxidize a range of aldehydes including reactive aldehydes was
134 compared to WT to get more insight into the function of AAO2. The crude protein extracted
135 from the rosette leaves of *aao2 KO* (KO-95) and WT was fractionated by NATIVE PAGE.

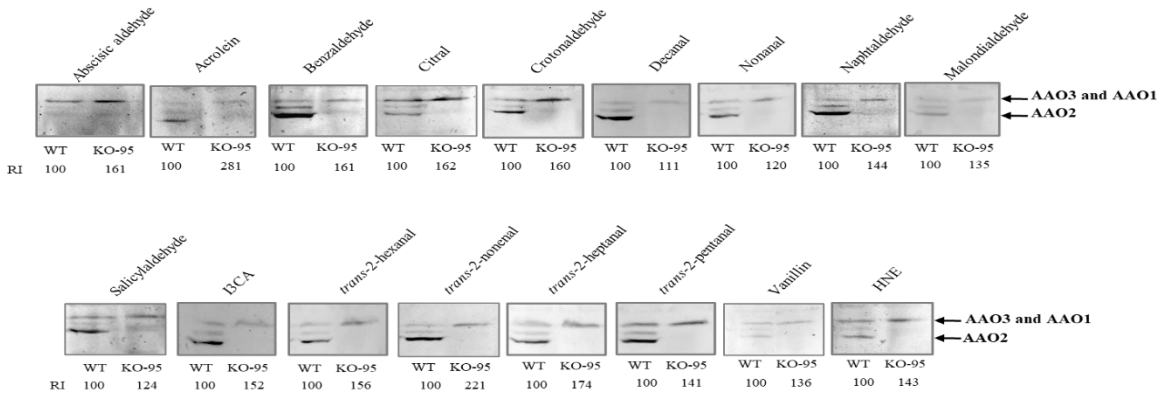

136

Figure 2. *Arabidopsis* aldehyde oxidases (AAOs) activity assessment in WT and *aao2* [SALK104895 (KO-95)] mutant using different aldehydes as the substrate. One hundred µg protein extracted from rosette leaves of 23-day old WT and KO-95 mutant plants were fractionated by NATIVE PAGE and AO activity with indicated aldehyde as the substrate was carried out. AO enzyme activity was determined in a reaction solution containing 100 mM Tris-HCl (pH 7.5), 1 mM 3-(4,5-dimethylthiazol-2-yl)-2,5-diphenyltetrazolium bromide, 0.1 mM phenazine methosulfate and 1 mM aldehydes, except for HNE and abscisic aldehyde that were applied with 0.25 mM and 0.1 mM, respectively. The reaction was stopped after 3h and after 2 h for abscisic aldehyde, by immersing the gel in 5% acetic acid solution. Thereafter gel images were captured and analyzed for relative intensity (RI) using ImageJ software (http://imagej.nih.gov/ij/) for the slowest (uppermost) migrated band intensity compared to the WT uppermost migrated band as reference (100%).

137 Significantly, knockout of *aao2 KO(KO-95)* mutant exhibited only the upper activity band,
138 whereas WT exhibited additional middle and the lowest activity bands (Fig.1C and Fig.2). The

application of various aldehydes at the level of 1 mM [except for HNE (0.25 mM) and ABal (0.1mM)] exhibited that upper in-gel activity band generated by *aao2 (KO-95)* extracted proteins had a more intense activity band (higher activity level) with almost all aldehydes employed as substrates as compared with WT. These results indicate that the absence of AAO2 enhances the oxidation capacity of aldehydes (Fig. 2), suggesting a role for AAO2 in the homeostasis of aldehydes level by modulating another/other aldehyde oxidase/s activity in plant leaves.

UV-C irradiation results-in a faster aldehyde induced senescence in WT compared to *aao2* mutants.

The generation of toxic aldehydes which leads to plant senescence is a major response of plants exposed to abiotic stresses. Among the abiotic stresses, UV-C was shown recently to induce

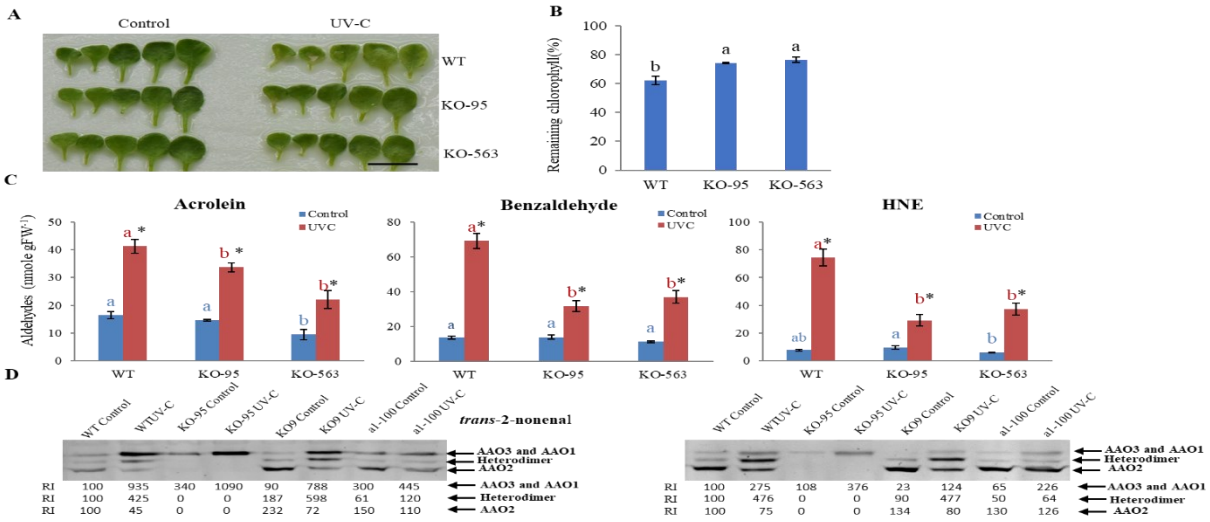

Figure 3. Determination of UV-C-irradiation-induced senescence and senescence-related factors in rosette leaves of *Arabidopsis* wild-type (WT) and *aao2* KO [SALK_104895 (KO-95) and SAIL_563_G09 (KO-563)] mutant plants. **A.** Representative photograph of WT and *aao2* rosette leaves in response to UV-C irradiation. 21-day post germination plants exposed to 250 mJ of UV-C irradiation were kept in a growth room for 72 hours and thereafter documented. Scale bar=1 cm. Rosette leaves were collected 3 days after UV-C treatment and rosette leaves of plants that were not exposed to UV-C were used as the control. First five leaves, oldest to youngest, from left to right are presented. **B.** Remaining chlorophyll in leaves after UV-C treatment. **C.** Indicated aldehyde profiling in control (blue bars) and UV-C treated (red bars) plants. Leaves from 3 different plants were taken as one replica and the bars show the average of at least 4 replicas. Different letters above the bar indicate significant differences (Tukey-Kramer HSD test, P<0.05). Asterisk shows significant differences between treatments within the same genotype (Student's t test, P < 0.05). **D.** Aldehyde oxidases (AAOs) in gel activity in control and UV-C treated WT, *aao2* (KO-95), *aao3* [SAIL_78_H09 (KO9)] and *aao1* [SALK_018100 (a1-100)]. 150 µg crude protein extracted from rosette leaves were fractionated by NATIVE PAGE and were used for the in-gel activity, assayed for 1h in solution containing 100 mM Tris-HCl (pH 7.5), 1 mM 3-(4,5-dimethylthiazol-2-yl)-2,5-diphenyltetrazolium bromide, 0.1 mM phenazine methosulfate and 1 mM *trans*-2-nonenal or Benzaldehyde as the aldehyde substrate. The gels were scanned, and intensity of the activity bands was estimated using ImageJ software (http://imagej.nih.gov/ij/) and compared with the intensity obtained with UV-C untreated (control) WT (employed as 100%) and presented as relative intensity (RI).

151 premature senescence of siliques and rosette leaves in *Arabidopsis* by enhancing the generation
152 of toxic aldehydes (Srivastava et al. 2017; Nurbekova et al. 2021). Interestingly, a decreased
153 transcript expression of AAO2, as well as declined AAO2 activity but enhanced activity of the
154 middle activity band that contains AAO2 [heterodimer of AAO2 with AAO1 or AAO3 (Akaba
155 et al. 1999; Koiwai et al. 2004)] in leaves was noticed in WT as well as *aao1* and *aao3* mutants
156 exposed to UV-C irradiation (Supplemental Fig. S1). Thus, it was reasonable to study how UV-
157 C irradiation will affect *aao2KO* mutant in the absence of AAO2. Notably, the application of
158 250 mJ of UV-C irradiation resulted in earlier senescence and greater chlorophyll loss in WT
159 leaves as compared to the two *aao2 KOs (KO-95 and KO-563)* mutants three days after the
160 application of the UV-C irradiation (Fig.3A and B). Determination of the aldehyde level in
161 UV-C treated plants revealed significantly higher levels of acrolein, benzaldehyde and HNE in
162 WT than in the leaves of *aao2 KO* mutant (Fig.3C). An in-gel assay that was carried out to
163 examine the AAO3 and AAO1 activity levels in control (UV-C untreated) and in UV-C treated
164 WT, *aao2KO, aao3KO* (containing active AAO1 and AAO2) and *aao1KO* (containing active
165 AAO3 and AAO2) mutants. Using *trans*-2-nonenal or benzaldehyde as the substrates, revealed
166 enhanced intensity in the most upper (least migrated) activity band in *aao2* mutant compared
167 to WT, *aao1KO* and *aao3KO,* indicating that the absence of active AAO2 enhances the activity
168 of AAO1 and AAO3. The UV-C irradiation resulted in enhancement of the uppermost band in
169 all genotypes tested, indicating the activation of AAO1 and AAO3 in the absence and presence
170 of AAO2 activity. Examination of AAO1 in *aao3* and AAO3 activity in *aao1* mutant revealed
171 that both enzyme activities were enhanced with both aldehyde substrates used, as the result of
172 UV-C irradiation (Fig.3D). Parallel to AAO1 and AAO3 increase, the heterodimer's activity
173 bands [middle bands (Akaba et al. 1999; Koiwai et al. 2004)] in WT
174 (AAO1:AAO2+AAO3:AAO2) and *aao3* mutant (AAO1:AAO2) exhibited higher increase in
175 response to the applied stress than the heterodimer activity in *aao1* mutant (AAO3:AAO2) with
176 either aldehyde substrate used (Fig.3D). Notably, the AAO3 and/or AAO1 enhanced activity
177 in plants exposed to UV-C irradiation was followed by AAO2 activity (most migrated band)
178 decrease in WT, *aao1KO* and *aao3KO* plants. Accordingly, the absence of AAO2 in *aao2KO*
179 plant resulted in higher activity of AAO3 and/or AAO1, and thus a better aldehyde
180 detoxification and reduced chlorophyll degradation (Fig.3A-D).

181 **Application of Rose Bengal confers aldehyde induced earlier senescence in WT**
182 **compared to *aao2* mutant leaves.**
183

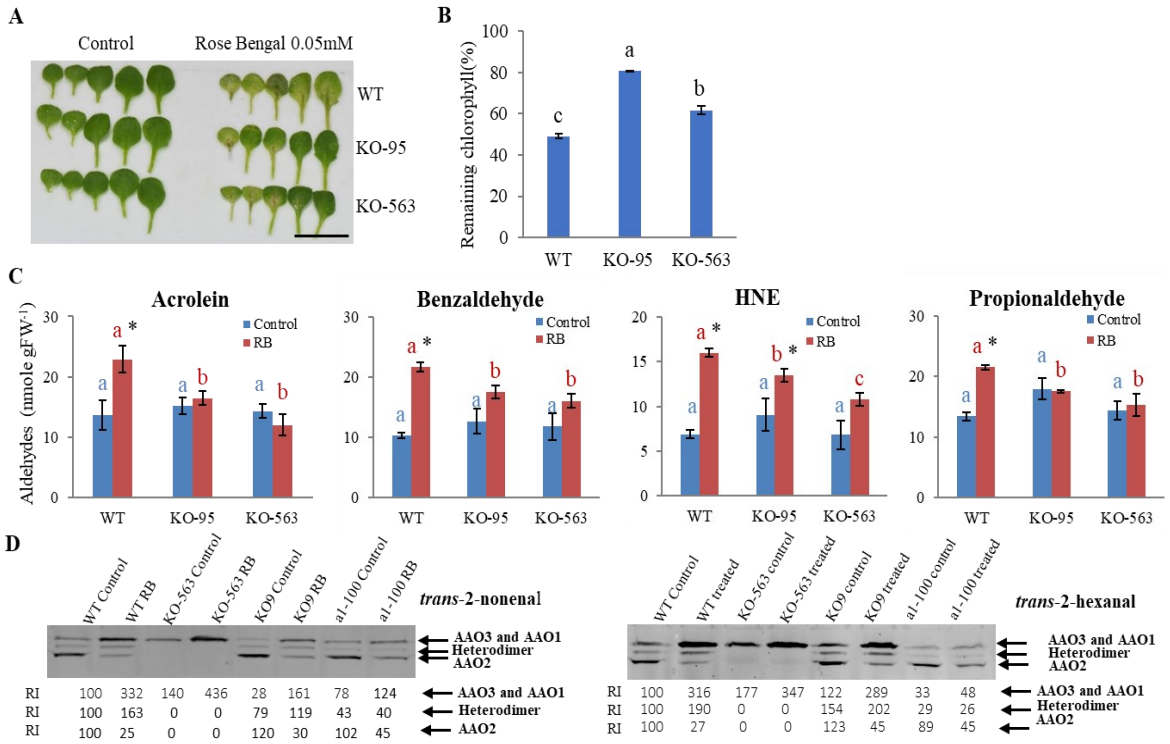

Figure 4. Determination of Rose Bengal-induced senescence and senescence-related factors in rosette leaves of *Arabidopsis* wild-type (WT) and *aao2* KO [SALK_104895 (KO-95) and SAIL_563_G09 (KO-563)] mutant plants. **A.** Representative photograph of WT and *aao2* rosette leaves in response to Rose Bengal application. 23 days post germination plants treated with 0.05 mM Rose Bengal were kept in a growth room for 72 hours and thereafter documented. Scale bar=2 cm. First five leaves, oldest to youngest, from left to right are presented. The rosette leaves were collected 17 hours after Rose Bengal treatment and rosette leaves of plants that were not exposed to Rose Bengal were used as the control. **B.** Remaining chlorophyll in first five leaves after Rose Bengal treatment. **C.** Indicated aldehyde profiling in control (blue bars) and Rose Bengal treated (red bars) plants. Leaves from 3 different plants were taken as one replica and the bars show the average of at least 4 replicas. Different letters above the bar indicate significant differences (Tukey-Kramer HSD test, $P<0.05$). Asterisk shows significant differences between treatments within the same genotype (Student's t test, $P < 0.05$). **D.** Aldehyde oxidases (AAOs) in gel activity in control and Rose Bengal treated WT, *aao2* (KO-95), *aao3* [SAIL_78_H09 (KO9)] and *aao1* [SALK_018100 (a1-100)]. 150 µg crude protein extracted from rosette leaves were fractionated by NATIVE PAGE and were used for the in-gel activity, assayed for 1h in solution containing 100 mM Tris-HCl (pH 7.5), 1 mM 3-(4,5-dimethylthiazol-2-yl)-2,5-diphenyltetrazolium bromide, 0.1 mM phenazine methosulfate and 1 mM *trans*-2-nonenal or *trans*-2-Hexanal as the aldehyde substrate. The gels were scanned, and intensity of the activity bands was estimated using ImageJ software (http://imagej.nih.gov/ij/) and compared with the intensity of the activity band obtained with Rose Bengal untreated (control) WT (employed as 100%) and presented as relative intensity (RI).

Rose Bengal is a well-known singlet oxygen generator (Knox and Dodge, 1984; Havaux and Triantaphylide, 2009) that participate in lipid peroxidation resulting in the generation of toxic aldehydes that above a certain level can lead to programmed cell death (Triantaphylidès et al. 2008). Applying 0.05 mM Rose Bengal by spray, as another abiotic stress type, induced early senescence symptoms in rosette leaves of WT three days after treatment, whereas *aao2* leaves showed much less visible senescence symptoms (Fig.4A). Detection of the remaining chlorophyll revealed a significant chlorophyll degradation in leaves of WT three days after Rose Bengal application, whereas the chlorophyll was less degraded in *aao2* leaves (Fig.4B).

193 Detection of aldehydes 17 h after Rose Bengal application revealed higher enhancement of
194 acrolein, benzaldehyde, propionaldehyde and HNE in WT than in the leaves of the 2 *aao2*
195 mutants (Fig.4C). In-gel AAO activity assay carried out to examine the AAO3 and AAO1
196 activity levels in the control treated WT and *aao2* mutant using *trans*-2-nonenal or *trans*-2-
197 hexanal as the substrate, revealed higher activity band intensity in the most upper activity band
198 in *aao2* mutant compared to WT. Using *trans*-2-nonenal as the substrate revealed higher AAO3
199 activity than AAO1 under control conditions, as indicated by the higher intensity in the most
200 upper band in *aao1* compared to *aao3* mutant. In contrast, *trans*-2-hexanal was a preferable
201 substrate for AAO1 activity, as indicated by the higher intensity of the most upper band in *aao3*
202 compared to *aao1* mutant. The application of Rose Bengal resulted in enhancement of the
203 uppermost band in WT and all examined mutants, indicating the activation of AAO1 and/or
204 AAO3 in the absence and presence of AAO2 activity. Examination of AAO1 in *aao3* and
205 AAO3 activity in *aao1* mutant exposed to Rose Bengal revealed that both enzyme activities
206 were enhanced with either aldehyde substrate used (Fig.4D). Interestingly, the heterodimer
207 activity bands in WT (AAO1:AAO2 and AAO3:AAO2) and in *aao3* mutant (AAO1:AAO2)
208 exhibited an increase in response to the applied stress, whereas the heterodimer activity in *aao1*
209 mutant (AAO3:AAO2) tended to show the absence of enhanced intensity with either aldehyde
210 substrate used (Fig.4D). Notably, similar to the UV-C treatment (Fig. 3D), the AAO3 and/or
211 AAO1 enhanced activity in plants exposed to Ros Bengal spray was followed by AAO2
212 activity decrease in WT, *aao1KO* and *aao3KO* plants. Accordingly, the absence of AAO2 in
213 *aao2KO* plant resulted in higher activity of AAO3 and/or AAO1, and thus a better aldehyde
214 detoxification and reduced chlorophyll degradation (Fig. 4A-D).

215

216 **The absence of active AAO2 enhances tolerance to UV-C irradiation and Rose Bengal**
217 **application by improving the capacity of AAO3 to detoxify aldehydes.**

218 The higher resistance of *aao2* KO mutants compared to WT exposed to UV-C irradiation and
219 Rose Bengal application prompted us to examine the possible role of each of the two enzymes:
220 AAO1 and AAO3, in the improved tolerance to the stresses by generating single functioning
221 mutants. The generation of single functioning *aao1* (*aao1S*) was done by silencing *AAO3* in
222 the background of *aao2* (KO-95), while *aao3S* was generated by silencing *AAO1* in the
223 background of *aao2* (KO-95) or *AAO2* silencing in the background of *aao1* KO mutant. The
224 AAO-compromised lines were exposed to UV-C irradiation or Rose Bengal spray after

225 verifications of the mutations by detection of the transcript's expression of the targeted genes
226 as compared to the expression in WT leaves (Supplemental Fig. S2).

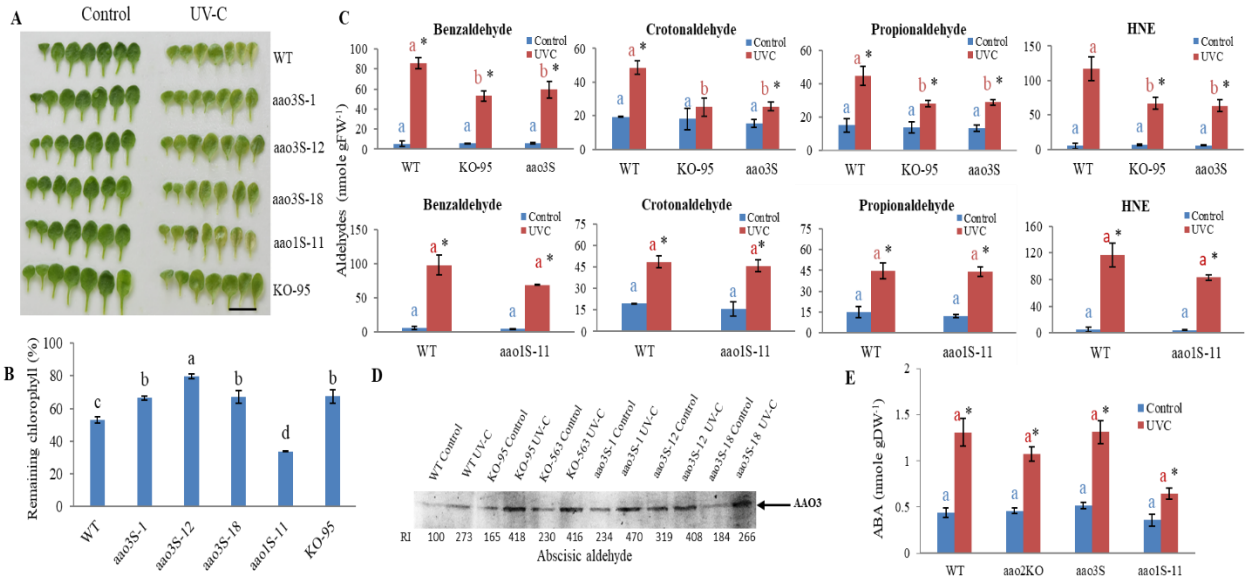

227

Figure 5. Determination of UV-C-irradiation-induced senescence and senescence-related factors in rosette leaves of *Arabidopsis* aldehyde oxidases single mutants *[aao1Single (aao1S)* and *aao3Singles (aao3S)*], *aao2* KO [SALK_104895 (KO-95) and wild-type (WT) plants. **A.** Representative photograph of WT, *aao2, aao1S* and *aao3S1 (aao3S-1, aao3S-12, aao3S-18)* rosette leaves in untreated (control) and UV-C irradiation treated plants. 21-days post germination (DPG) plants exposed to 250 mJ of UV-C irradiation were kept in a growth room for 72 hours and thereafter documented together with rosette leaves of plants not exposed to UV-C (control). Scale bar=2 cm. **B.** The level of remaining chlorophyll in the first seven leaves (oldest to youngest from left to right) after exposing WT and the various mutant plants to UV-C treatment. **C.** Indicated aldehyde profiling in control (blue bars) and UV-C treated (red bars) plants. Leaves from 3 different plants were taken as one replica and the bars show the average of at least 4 replicas. *aao3S* represents the average of the 3 independent *aao3* single mutants. **D.** Aldehyde oxidase 3 (AAO3) in gel activity in control and UV-C treated WT, *aao2* [KO-95), SAIL_563_G09 (KO-563)] and *aao3S (aao3S-1, aao3S-12, aao3S-18)* using abscisic aldehyde as the specific substrate for AAO3. 150 µg crude protein extracted from WT, *aao2* (KO-95 and KO-563) and *aao3S (aao3S-1, aao3S-12, aao3S-18)* rosette leaves were fractionated by NATIVE PAGE and were used for activity. The gels were scanned after 30 min, and intensity of the activity bands was estimated using ImageJ software (http://imagej.nih.gov/ij/) and compared with that obtained with UV-C untreated (control) WT (employed as 100%) and presented as relative intensity (RI). **E.** Abscisic acid (ABA) level in rosette leaves of WT, *aao2KO (KO-95, KO-563), aao1S (aao1S-11)* and *aao3S* (*aao3S-1, aao3S-12, aao3S-18*) untreated control (blue bars) and UV-C treated (red bars) plants. Different letters above the bar indicate significant difference (Tukey-Kramer HSD test, P<0.05). Asterisk shows significant differences between treatments within the same genotype (Student's t test, P < 0.05).

228 Notably, rosette leaves of the *aao1S (aao1S-11)* mutants impaired in AAO3 and AAO2
229 expressions exhibited significantly lower remaining chlorophyll level than WT leaves 3 days
230 after exposing to 250 mJ of UV-C irradiation or 0.05 mM of Rose Bengal application. In
231 contrast, *aao3S* mutants *(aao3S-1, aao3S-7, aao3S-12, aao3S-18)* impaired in AAO1 and
232 AAO2 expression, as well as the *aao2* (KO-95) mutant exhibited significantly higher remaining
233 chlorophyll level than WT in response to the applied stresses (Fig.5A, B and Fig.6A, B).
234 Further, detection of aldehydes level in rosette leaves was carried out 3 days after the UV-C
235 irradiation, and revealed significantly higher level of benzaldehyde, crotonaldehyde,

236 propionaldehyde and HNE in WT leaves compared to *aao2 KO* and the three *aao3S (aao3S-1,*
237 *aao3S-12, aao3S-18)* mutants. In contrast, the levels of these aldehydes in *aao1S* mutant leaves
238 were similar to those in WT (Fig.5C). Detection of aldehydes content in leaves 17h after Rose
239 Bengal application revealed significantly higher accumulation of acrolein, benzaldehyde and
240 HNE in WT and *aao1S* mutant leaves than in leaves of *aao2* (KO-95) and the *aao3S (aao3S-*
241 *7, aao3S-12, aao3S-18)* mutants (Fig.6C).

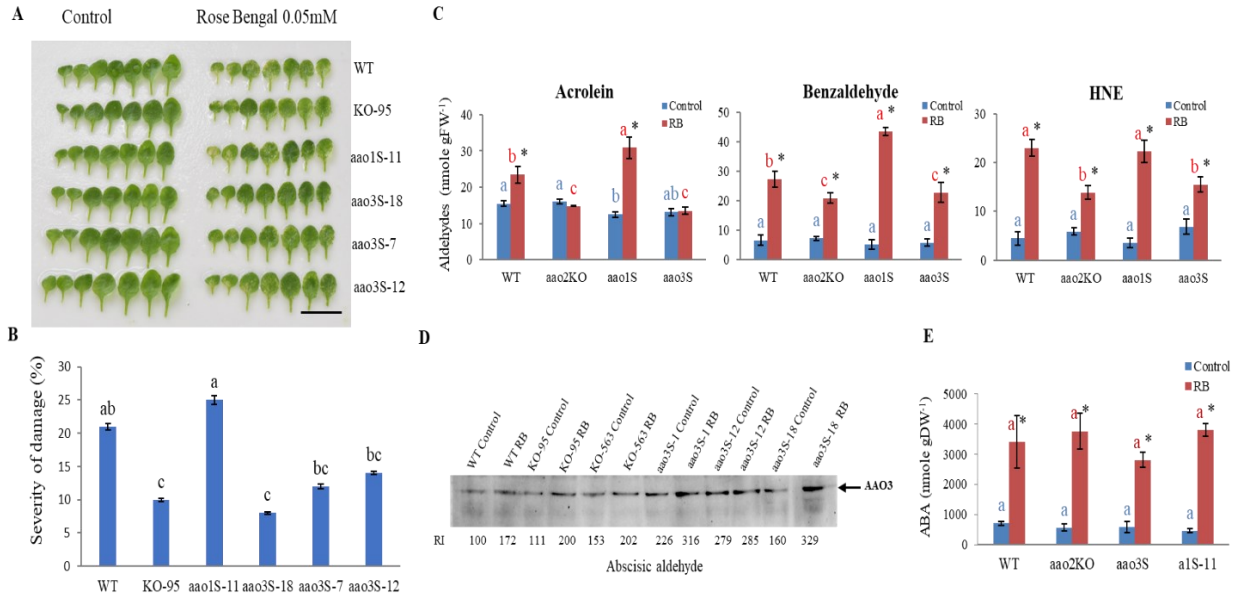

242

Figure 6. Determination of Rose Bengal-induced senescence and senescence-related factors in rosette leaves of *Arabidopsis* aldehyde oxidases single mutants *[aao1Single (aao1S)* and *aao3Singles (aao3S)*], *aao2* KO [SALK-_104895 (KO-95) and wild-type (WT) plants. **A.** Representative photograph of WT, *aao2, aao1S* and *aao3S2 (aao3S-7, aao3S-12, aao3S-18)* rosette leaves in untreated (control) and Rose Bengal treated plants. 21-DPG plants treated with 0.05 mM of Rose Bengal were kept in a growth room for 72 hours and thereafter documented. Scale bar=2 cm. **B.** Damage level in leaves as shown in (A) was calculated as described in the materials and methods. Means +-SEM (n = 6). **C.** Indicated aldehyde profiling in control (blue bars) and Rose Bengal treated (red bars) plants. Seventeen hours after Rose Bengal treatment leaves from 3 different untreated (control) or treated plants were taken as one replica and the bars show the average of at least 4 replicas. *aao3S* is average of the 3 independent *aao3* singles plants. **D.** Aldehyde oxidases 3 (AAO3) in gel activity in control and Rose Bengal treated WT, *aao2* [KO-95), SAIL_563_G09 (KO-563)] and *aao3S* using abscisic aldehyde as the specific substrate for AAO3. 150 µg crude protein extract from WT, *aao2 (*KO-95, KO-563*)* and *aao3S* rosette leaves was fractionated by NATIVE PAGE and were used for the in-gel activity. The gels were scanned after 1h, and the intensity of the activity bands was estimated using ImageJ software (http://imagej.nih.gov/ij/) and compared with that obtained with Rose Bengal untreated (control) WT (employed as 100%) and presented as relative intensity (RI). **E.** ABA content in rosette leaves of WT, *aao2KO (KO-95, KO-563), aao1S (aao1S-11)* and *aao3S* (*aao3S-7, aao3S-12, aao3S-18*) untreated control (blue bars) and Rose Bengal treated (red bars). Different letters above the bar indicate significant differences (Tukey-Kramer HSD test, P<0.05). Asterisk shows significant differences between treatments within the same genotype (Student's t test, P < 0.05).

243 To further rule out the possible role of AAO1 in *aao2* resistance to the applied stresses, *AAO1*
244 overexpression mutant (*A1OE*) used by us before [Nurbekova et al. 2021 (Fig.1B and C)], was
245 exposed together with WT plants to UV-C irradiation that revealed a higher chlorophyll
246 degradation in A1OE (Supplemental Fig. S3A and B). Additionally, similar levels of
247 benzaldehyde, crotonaldehyde, HNE and higher levels of propionaldehyde in *A1OE* compared

248 to WT were detected (Fig. 3C). The results show better resistance of *aao2* KOs and *aao3S*
249 mutants than WT, whereas *aao1S* and *A1OE* mutants exhibited similar resistance to WT when
250 exposed to the abiotic stresses applied (Figs 5A-C, 6A-C, Supplemental Fig. S3). This indicates
251 that AAO1 did not play a role in stress improved resistance of *aao2 KO* as compared to WT
252 while AAO3 is the major player in the detoxification of reactive aldehydes in the absence of
253 active AAO2 in *aao2 KOs*. Additional support to this notion was demonstrated by employing
254 ABal as the indicator substrate specific for AAO3 In-gel activity (Akaba et al. 1998, 1999;
255 Koiwai et al. 2004; Koshiba et al. 1996; Omarov et al. 1999; Seo et al. 2000a,b; Srivastava et
256 al. 2017; Nurbekova et al. 2021) that exhibited higher AAO3 activity level in response to UV-
257 C or Rose Bengal application in all the included genotypes, being significantly higher than WT
258 in *aao2 KO* and *aao3S* mutants. This result indicates that AAO3 is more active in the absence
259 of active AAO2 in *aao2 KO* and *aao3S* mutants compared to WT under the stresses applied
260 (Fig.5D and Fig.6D). Further detection of the ABA level revealed similar enhancement levels
261 in WT compared to *aao2 KO*, *aao3S* and *aao1S* mutants exposed to UV-C irradiation or Rose
262 Bengal application, supporting the notion that the AAO3 - enhanced detoxification activity of
263 aldehyde, rather than ABA level played a role in *aao2 KO* better resistance than in WT and
264 *aao1* mutant (Fig.5E and Fig.6E).
265 To examine if indeed *aao2KO* mutants can better resist toxic levels of aldehydes than WT,
266 plants were exposed to 4.5 mM benzaldehyde as done recently (Nurbekova et al. 2021) and
267 revealed higher chlorophyll degradation in WT than in the two independent mutants' leaves 72
268 h after aldehyde application (Supplemental Fig. S4A and B). These results further indicate the
269 higher capacity of *aao2* KO mutants than WT to protect leaves from aldehyde induced
270 chlorophyll degradation.
271
272 **DISCUSSION**
273
274 **The absence of active AAO2 improves AAO3's capacity to protect plants from UV-C and**
275 **RB induced chlorophyll degradation.**
276 Early observations showed the presence of three AAO genes in leaves and their
277 expression dependency on the developmental stage and applied abiotic stresses. *Arabidopsis*
278 AAO1 was shown to be mainly expressed in seedlings and rosette leaves (Seo et al. 2000a;
279 Koiwai et al. 2004), oxidizing indole-3-carboldehyde (ICHO) to indole-3-carboxylic acid
280 [ICOOH ((Bottcher et al. 2014))]. AAO3 was shown to be expressed in seedlings and rosette
281 leaves (Seo et al. 2000a; Koiwai et al. 2004), oxidizing abscisic aldehyde (ABal) to abscisic

282 acid (ABA) (Seo et al. 2000a, 2000b;) as well as protecting rosette leaves from stress induced
283 aldehyde toxicity by oxidizing the toxic aldehydes (Nurbekova et al. 2021). The roles of AAO2
284 are not known and thus require further study. In the current study it was shown that exposing
285 WT and *aao2* mutants, as well as *aao1S* and *aao3S* mutants to UV-C irradiation or Rose Bengal
286 spray revealed enhanced senescence induced by endogenously generated higher level of
287 benzaldehyde, HNE and acrolein in WT and *aao1S* compared to *aao3S and aao2 KOs* mutant's
288 leaves (Fig.3A-C, Fig.4A-C, 5A-C and 6A-C). These results indicate the essentiality of the
289 absence of active AAO2 and the presence of active AAO3, whereas the presence of active
290 AAO1 is not essential for the better stress resistance genotypes, the *aao2KO*, and the single
291 mutants of *aao3S* under applied stress conditions. The lower remaining chlorophyll content
292 and higher level of propinaldehyde and similar enhacement in benzaldehyde, crotonaldehyde
293 and HNE levels in AAO1OE compared with WT upon UV-C irradiation, further ruled out a
294 possible involvement of AAO1 in *aao2* KO better resistance than WT (Supplemental Fig. S3).
295 Employing In-gel AO assay with ABal as a specific substrate marker for AAO3 activity
296 showed higher AAO3 activity in *aao2 KOs* and *aao3Ss* as compared to WT leaves treated with
297 UV-C or Rose Bengal (Fig.5D and Fig.6D), indicating that enhanced AAO3 capacity plays a
298 role in *aao2KOs* and *aao3Ss* better resistance.
299 The involvement of reactive aldehydes in stress-induced damage to plants was
300 previously reported, and among lipid peroxide derived carbonyls, α, β-unsaturated aldehydes
301 such as HNE, acrolein and crotonaldehyde were identified as the most reactive species
302 (Yamauchi et al. 2008; Mano et al. 2010, Mano et al. 2014; Srivastava et al. 2017).
303 Interestingly, higher levels of benzaldehyde, acrolein, propionaldehyde and crotonaldehyde
304 were shown to induce early senescence in *aao3* leaves when exposed to UV-C irradiation.
305 Similar to the experimental condition in the current study, *aao3* plants, known as ABA
306 deficient mutants, were grown on half-strength MS media in agar plates sealed with surgical
307 tapes, to control any drought involvement in senescence level in WT and *aao3* mutant
308 (Nurbekova et al., 2021). Indeed, under such controlled condition no effect of ABA or drought
309 stress related was noticed in the *aao3* plants (Nurbekova et al. 2021), whereas similar level of
310 ABA was evident in WT, *aao2KOs, aao1S* and *aao3Ss* in control and stressed plants (Fig.5E
311 and Fig.6E). To support the levels of ABA detected in the stressed plants the expression of
312 *NCED3-2* gene was examined in the leaves of the control and the UV-C or Rose Bengal
313 stressed plants. Considering that *NCED3-2* gene product acts as the commited step of ABA
314 biosynthesis (Ruggiero et al. 2020) generating xanthoxin that leads to the biosynthesis of
315 ABAld, the substrate of AAO3 (Sussmilch et al. 2017), the similar transcript expression of

316 *NCED3-2* evident in WT and *aao2KOs* and *aao3Ss* exposed to the applied stresses
317 (Supplemental Fig. S5), is in agreement with the similar levels of ABA detected in the stressed
318 genotypes. These results indicate that not the ABA level but rather the activated AAO3 is
319 reponsible for the higher level of the remaining chlorophyll by better aldehyde detoxification
320 capacity in *aao2KOs* and *aao3Ss* mutant plants exposed to UV-C irradiation or Rose Bengal
321 application (Fig.5D and Fig.6D).
322
323 **The absence of active AAO2 in *aao2 KO* mutants enhances AAO3 activity as the**
324 **result of improved sulfuration by ABA3.**
325 The decrease in AAO2 activity in WT as well as the *aao1* and *aao3* mutants exposed to UV-C
326 or Rose Bengal (Figs. 3D, 4D), and specifically the higher AAO3 activity than in WT, in the
327 mutants absent active AAO2, the *aao2 KOs* and *aao3S*s, grown with or without those stress
328 conditions (Figs. 5D, 6D), led us to examine the reason/s for such phenomenon. It is possible
329 that the absence of AAO2 likely leads to higher availability of MoCo and/or less competition
330 for MoCo sulfuration, resulting in increased activity in the upper activity band that includes
331 AAO3 and AAO1 in WT and aao*2 KOs* and only AAO3 in the *aao3Ss.*
332 In-vitro sulfuration of AO by employing Na_2S under anaerobic reducing conditions was
333 previously demonstrated in leaves and roots of WT, recovering significantly the AO activity in
334 the tomato Moco sulfurase (*flacca*) mutant roots and leaves (Sagi et al. 1999), as well as in
335 *aba3* mutant, by employing L-Cysteine (Bittner et al., 2001; Mendel, 2022). Similarly, in-vitro
336 sulfuration was applied and in-gel activity assay of AAO using *trans*-2-nonenal as the substrate
337 was carried out to examine AAO activity levels in the control and the sulfurated extracts of
338 WT, *aao2KO* and *aba3* leaves. Interestingly the uppermost activity band, containing enzyme
339 activities of AAO1 and AAO3 (Nurbekova et al. 2021) was enhanced by 40% in control treated
340 *aao2 KO* mutant as compared to WT's most upper activity band. Notably, in-vitro sulfuration
341 of WT extracts resulted in a significant increase by 62% in AAO2 activity as well as more than
342 2-fold enhancement in the heterodimer middle activity band containing a monomer of AAO2,
343 while the uppermost activity band exhibited a slightly lower activity level than the control when
344 *trans-2*-nonenal was used as the substrate. In contrast, the in-vitro sulfuration in *aao2KO* was
345 almost 2-fold higher than in the sulfurated WT and 41% higher than the activity in the *aao2KO*
346 control extract (Supplemental Fig. S6A). These results indicate that AAO2, as the homodimer
347 (lowest migrated activity band) as well as the heterodimer (middle migrated activity band)
348 targets the majority of the sulfuration as compared to the upper activity band (Supplemental
349 Fig. S6A). In support of this notion, employing in-vitro sulfuration in *aba3* mutant that lacks

350 AAO activities led to more than 2-fold higher intensity of AAO2 activity as compared to the
351 heterodimer and the most upper activity bands of the sulfurated extract in *aba3* mutant
352 [calculated using the intensities of the activity bands in *aba3* Supplemental Fig. S6A)].
353 Importantly, the results indicated that the artificial sulfuration process used partially but
354 significantly recovered AAO activities, as it was ca 60%, 90% and 50% in the upper, middle,
355 and the lowest activity band as compared to the non-sulfurated extract of WT leaves,
356 respectively (Supplemental Fig. S6A).

357 ABal that was shown as the specific substrate for AAO3 among the four aldehyde
358 oxidases in *Arabidopsis* (Akaba et al. 1998, 1999; Koiwai et al. 2004; Koshiba et al. 1996; Seo
359 et al. 2000a, b) was used to identify the responses of AAO3 to the sulfuration process, as one
360 of the 2 enzymes responsible for the most upper activity band. Notably, while the sulfuration
361 process recovered a faint AAO3 activity band in sulfurated *aba3* that was ca 11% of the activity
362 detected in non-sulfurated WT under control conditions, the sulfuration of *aba3* after UV-C
363 irradiation enhanced AAO3 activity by more than 5-fold (Supplemental Fig. S6B), indicating
364 that UV-C irradiation most likely enhanced the level of inactive unsulfurated AAO3 in *aba3*
365 mutants. Since UV-C irradiation and environmental stress such as Rose Bengal spray were
366 shown to enhance the relative expression of *ABA3* transcription in WT and *aao2 KOs*
367 (Supplemental Fig. S7A and B) as well as the expression of *AAO3* transcript in WT but not in
368 *aao2 KO* mutants (Supplemental Fig. S8) it is likely that UV-C will enhance the levels of active
369 AAO3, at least in the *aao2 KO* mutants mainly by sulfuration of inactive AAO3 proteins.

370 While control treated plants revealed 2.5-fold higher AAO3 activity in *aao2 KO* mutant
371 compared to WT, the sulfuration process enhanced AAO3 activity in WT by 89% and in *aao2*
372 *KO* by 37%, the latter still being higher than WT by 81%. Treating the control WT and *aao2*
373 *KO* plants with UV-C irradiation resulted in higher AAO3 activity increase than the sulfuration
374 process, as the activity was enhanced by more than 4-fold in WT and more than 2-fold in *aao2*
375 *KO*, being still higher by 11% in the latter (Supplemental Fig. S6B). Notably, trying to enhance
376 AAO3 activity by applying the sulfuration process to UV-C treated plants revealed 18%
377 increased activity in WT and 14% in *aao2 KO*, the latter was still higher by 8% than in WT.
378 These results indicate that while environmental stresses such as UV-C irradiation likely
379 enhance the level of active AAO3 in both WT and the *aao2KO*, the active AAO2 in WT
380 employs a sulfuration process essential for AAO3 activation, resulting in higher availability of
381 activation by sulfuration of the AAO3 in *aao2 KO* compared to AAO3 in WT.

382

383 **Summary**

384 The current study demonstrates that AAO2 activity level oppositely affects AAO3
385 activity, while mutation of AAO2 expression better delays plant senescence by AAO3-
386 enhanced aldehyde detoxification activity in plants exposed to UV-C irradiation or Ros-Bengal
387 spray (Figs. 1C-6). Firstly, it was shown that *aao2KO* can detoxify an array of reactive
388 aldehydes by higher activity than in WT of AAO1 or AAO3 or both exposed to UV-C
389 irradiation or Ros Bengal spray. Additionally, it was shown that AAO3 and/or AAO1 activity
390 increase was followed by AAO2 activity decrease in WT, *aao1KO* and *aao3KO* plants (Figs.
391 3-4). Secondly, an essential interplay between AAO2 and AAO3 in the regulation of
392 senescence level and carbonyl aldehyde detoxification under the stress conditions was
393 presented. Notably, the delayed senescence and the lower toxic aldehyde levels in *aao2KO* and
394 *aao3Ss* mutants, but not in WT, as well as in *aao1S* and *AAO1OE* mutants treated with UV-C
395 or Rose Bengal, demonstrate the essentiality of AAO2 impairment to plant senescence delay
396 by enhancing aldehyde detoxification activity by AAO3 (Figs.5-6). Finally, employing the
397 sulfuration process (known to activate aldehyde oxidases) in wild-type, *aao2KO*, and
398 *molybdenum-cofactor sulfurase* (*aba3-1*) mutant plants revealed that the active AAO2 in WT
399 employs sulfuration processes essential for AAO3 activity level, resulting in the lower AAO3
400 activity in WT than AAO3 activity in *aao2KO* (Supplemental Fig.6A and B). These results
401 demonstrate the essential role of AAO2 expression level in regulating AAO3 activity affecting
402 senescence delay in plant leaves by aldehyde detoxification.
403
404
405 **EXPERIMENTAL PROCEDURES**

406 **Chemicals**

407 Acrolein, benzaldehyde, cinnamaldehyde, citral, crotonaldehyde, decanal, dodecanal,
408 heptaldehyde, hexanal, *trans*-2-heptenal, 4-hydroxynonenal-dimethylacetal (HNE-DMA),
409 indole-3-carboxaldehyde, malondialdehyde [tetrabutylammonium salt], 1-naphthaldehyde,
410 nonanal, *trans*-2-nonenal, propionaldehyde, salicylaldehyde, *trans*-2-pentanal, *trans*-2-
411 hexanal, vanillin, diphenyltetrazolium bromide (MTT), phenazine methosulfate (PMS), were
412 purchased from Sigma Aldrich Chemical Company Inc. Abscisic aldehyde was purchased from
413 Toronto Research Chemicals (www.trc-canada.com).

414

415 **Plant material and growth conditions**

416 *Arabidopsis thaliana* var. Columbia wild type (WT), T-DNA homozygous knock out (KO)
417 lines for *AAO3* (At2g27150), SAIL_78_H09 (KO9), *AAO1* (At5g20960, SALK_018100), and
418 *AAO2*(At3g43600), KOs SALK_104895 (KO-95) and SAIL_563_G09 (KO-563) were
419 procured from ABRC (http://abrc.osu.edu/). *aba3-1* (At2g16540) used in this study used by
420 us before (Bekturova et al. 2021; Sagi et al. 2002) was procured from the same source.
421 Homozygous lines of T-DNA KOs were screened using PCR with the specific sets of primers
422 (Supplemental Fig. S1A and Supplemental Table *S*1A).
423 *aao1S* (*aao1* single) mutant was generated by silencing AAO3 in the background of *aao2* (KO-
424 95) and *aao3S* was generated by silencing AAO1 in the background of *aao2* and silencing and
425 AAO2 in the background of *aao1*. The expression of AAOs genes were quantified by qPCR
426 (Supplemental Fig. S2) in *aao1S*, *aao2S* and *aao3S* mutants by employing forward and reverse
427 primers localized to either side of the T-DNA insertion.
428 For the gene silencing we used the RNA interference system as done before (Brychkova
429 et al. 2007). The sense fragment was ligated into pRNA69 plasmid via the restriction sites XhoI
430 and EcoRI, and the antisense fragment through the restriction sites BamHI and XbaI. The
431 resulting construct was digested, and the fragment containing the 35S promoter and the inserted
432 AAO fragments was inserted via Not1 flanking sites of the binary vector pML-BART.
433 The generation of AAO1, AAO2 and AAO3 fragments for ligation into pRNA69
434 plasmid were generated as follows: Forward and reverse primers for the sense fragments were
435 attctcgagCGAGTTCTTCGGATCTTTA and gccgaattcAACATTCTGATCAAAACCA,
436 attCTCGAGTCTTGAGGCTCATGAT and attCTCGAGTCTTGAGGCTCATGAT,
437 attCTCGAGGAAAGAGAAGGTTGATAAT and aggGAATTCTGTTATGAAGCTCAG for
438 for AAO1, AAO2 and AAO3 respectively.
439 Forward and reverse primers for the antisense fragments were
440 GCCTCTAGACGAGTTCTTCGGATCTTTA and
441 ATAGGATCCAACATTCTGATCAAAACCA, attTCTAGATCTTGAGGCTCATGAT and
442 aggGGATCCTTCAGAGTTTGTTTCA, attTCTAGAGAAAGAGAAGGTTGATAAT and
443 aggGGATCCTGTTATGAAGCTCAG for AAO1, AAO2 and AAO3 respectively. The
444 construct was introduced into Agrobacterium tumefaciens strain GV3101 as described before
445 (Brychkova et al. 2007 and Srivastava et al. 2017) and transformed into the KO mutants using
446 the floral dip method (Clough and Bent,1998). Transformed *Arabidopsis* lines were first
447 selected by resistance to Basta® (glufosinate ammonium: Aventis CropScience
448 https://www.bloomberg.com) and verified by transcript expression level and sequencing.

449 Seeds were sown in Petri dishes containing half-strength MS medium supplemented
450 with 0.5% plant Agar (https://www.duchefa-biochemie.com/) and were placed at 4ºC for 2
451 days for stratification and then were grown at 14h light/10h darkness in a growth room, 22˚C,
452 with 75–85% relative humidity, and 100-150 µmol m^{-2} sec^{-1} as described in (Brychkova et al.
453 2007). Seven days post germination (DPG), the plants were transferred to 90 mm plates
454 containing half-strength MS medium supplemented with 0.5% sucrose and 1% agar. The
455 biomass of the rosette leaves was determined 3 or 4 days after UV-C irradiation or 17 hours
456 after spraying plants with RB. Untreated plants were used as the control.

457 **RNA isolation, cDNA preparation, and real-time PCR**

458 To quantify the transcripts using quantitative reverse transcriptase-polymerase chain reaction
459 (qPCR), total RNA was prepared by using the Aurum™ total RNA Mini Kit (Bio-Rad,
460 Hercules, CA) according to the manufacturer's instructions. The cDNAs were prepared in a
461 10µl volume containing 350 ng of plant total RNA that was reverse-transcribed with an
462 iScript™ cDNA Synthesis Kit using modified MMLV-derived reverse transcriptase (Bio-Rad),
463 a blend of oligo-d(T) and random hexamer primers according to the manufacturer's
464 instructions. The generated cDNA was diluted 10 times and the quantitative analysis of
465 transcripts was performed employing the sets of primers enlisted in Supplemental Table S2A
466 as described before (Brychkova et al. 2007; Oshanova et al. 2021).

467

468 **DNA sequence analysis**

469 Sequence analysis was performed with the ABI Prism Big Dye Terminator Cycle Sequencing
470 Ready Reaction Kit on an ABI Prism 310 cycle sequencer (PE Applied Biosystems,
471 Warrington, UK).

472 **Identification of unique peptides in activity bands**

473 To confirm the identity of the AAOs involved in the formation of the lower (most migrated)
474 bands in WT, *aao1* and *aao3* KO, during aldehyde oxidation (Fig. 1C), the activity bands were
475 excised from the native gel, and fractionated with 12% SDS-PAGE. Thereafter the proteins
476 were stained by Coomassie Brilliant Blue, and the individual lanes harboring stained bands
477 were cut from the gel and sent for peptide sequencing at The Smoler Protein Research Center
478 (https://proteomics.net.technion.ac.il/). The proteins were trypsinized and the resulting
479 peptides were separated by HPLC and analyzed by LC-S/MS on Q-Exactive (Thermo Fisher

480 Scientific). Data analysis was done as described in (Kurmanbayeva et al. 2017, Nurbekova et
481 al. 2021).

482

483 **Protein extraction and fractionation**

484 Soluble proteins were extracted from *Arabidopsis* rosette leaves as described before (Sagi et
485 al. 1998). Concentrations of total soluble protein in the resulting supernatant were determined
486 according to (Bradford et al. 1976). Native PAGE was carried out as follows; samples were
487 subjected to a Bio-Rad Mini-Protean III slab cell (Bio-Rad, Richmond, CA, USA), with a
488 discontinuous buffer system (Laemmli et.al 1970) in 7.5% (w/v) polyacrylamide separating
489 gels and 4% (w/v) stacking gels in the absence of SDS at 4° C. Tissue/buffer ratio was 1:3
490 (weight/volume). Extracted crude protein samples were centrifuged at 15000g for 20 min at
491 4ºC and then loaded to the gel after equalization of the proteins. The native-PAGE was carried
492 out using 1.5 mm thick slabs loaded with indicated levels of proteins.

493

494 **AAO In-gel activity**

495 AAO activity was tested using different aldehydes in 50mM Tris-HCl, pH 7.5, containing 1
496 mM 3-(4,5-dimethylthiazol-2-yl)-2,5-diphenyltetrazolium bromide (MTT), 0.1 mM phenazine
497 methosulfate (PMS) and one of various aldehydes (conc. is mentioned at the required places).
498 The reactions were stopped by immersion of the gels in 5% acetic acid. The quantity of
499 resulting formazan activity bands was directly proportional to enzyme activity during a given
500 incubation time, in the presence of excess substrate and tetrazolium salt (Rothe et al. 1974).
501 The gels were scanned, and the intensity of bands was determined using ImageJ software
502 (http://imagej.nih.gov/ij/).

503 **In vitro sulfuration of crude extracts**

504 In vitro sulfuration was carried out as previously described (Sagi et al. 1999; Sagi et al. 2002)
505 with slight modifications. Protein extraction of rosette leaves was done as described above in
506 the materials and methods section. The high heat stability of plant MoCo-containing
507 hydroxylases in plant leaves (Bower et al. 1978; Omarov et al. 1999; Sagi et al. 1999) allowed
508 to heat the resulted supernatant for 90 sec at 65 ºC and additionally centrifuge for 10 min at
509 4ºC as done previously (Nurbekova et al. 2021). Five hundred µl supernatant of the leave
510 extracts as well as one ml of extraction buffer passed through G-25 Sephadex that was

511 previously equilibrated with 6 ml extraction buffer and 1 ml of the desalted protein was
512 collected. For the sulfuration process 450 µl of the desalted protein incubated at room
513 temperature for 40 min together with 20.25 µl 0.1M dithionite, 17 µl of 0.5 M Na_2S, and 22.5
514 µl of 1.25 mM methyl viologen was the indicator of the reducing conditions, while gently
515 flushing N_2 through the mixture to maintain anaerobic conditions. A volume of 59.75 µl
516 extraction buffer was added to 450 µl desalted protein that served as the control. Proteins were
517 equalized before and after sulfuration and AO activity was detected in polyacrylamide gels by
518 stanning after native electrophoresis as previously described. Detection of AO activity was
519 carried out with desalted proteins extracted from WT, *aao2KO* and *aba3-1* mutant leaves.

520 **UV-C treatment**

521 UV-C treatment was applied by subjecting equal age plants (21 to 23 DPG) to 250 mJ UV-C
522 irradiation during 90 sec, using CL 508 Crosslinkers (UVITec Ltd, UK). WT, *aao2 (*KO-95 and
523 KO-563*)*, *aao1S(aao1S-11)* and *aao3S1(aao3S-1, aao3S-12, aao3S-18)* mutant plants, grown
524 in 1% agar plates containing half-strength MS media and 0.5% sucrose. UV-C irradiation-
525 treated and untreated (control) plants, were placed in the controlled growth room. Photographs
526 of the plants were taken 3 or 4 days after UV-C irradiation and the remaining plants were frozen
527 in liquid N and then stored at -80 ˚C for further use.

528 **Rose Bengal treatment in rosette leaves**

529 Twenty-three-day old *aao2* KOs SALK_104895 (KO-95) and SAIL_563_G09 (KO-563), WT,
530 *aao1S (aao1S-11)* and *aao3S2 (aao3S-7, aao3S-12, aao3S-18)* plants grown 3 plants per 90
531 mm plate were used for Rose Bengal treatment. Rose Bengal was dissolved using a magnetic
532 stirrer in DDW containing 0.01 % Silwet L-77. Fifty µM Rose Bengal was sprayed onto the
533 plates with 3 plants and the remaining solution was removed carefully, and plates were resealed
534 with surgical tape and kept 1 hour under the dark and then were transferred to the normal
535 growth room condition. DDW containing 0.01 % Silwet L-77 was used as the control. Plants
536 were sampled 17 h after Rose Bengal application. The effect of Rose Bengal treatment was
537 documented 72 h after the Rose Bengal application unless mentioned otherwise.
538

539 **Chlorophyll and leaf-damage level determination**

540 Total chlorophyll content was measured in extracts of the rosette leaves as described before
541 (Brychkova et al. 2008). The values for remaining chlorophyll content in rosettes were
542 determined as the quantity of chlorophyll per 20 mg for each sample divided by the quantity

543 of chlorophyll per 20 mg mock (control untreated) and were expressed as remaining
544 chlorophyll (%). The severity of leaf damage after Rose Bengal treatment was as follows: 0,
545 no damage; 1, 1-5%; 2, 6-10%; 3, 11–25%; 4, 26-40%; 5, >41% of leaf area damaged. The
546 average leaf damage was then multiplied by the total number of damaged leaves to determine
547 the level of damage.

548 **Determination and quantification of aldehydes, determination of aldehyde toxicity and**
549 **ABA determination.**

550 Aldehydes were determined according to Matsui et al. 2009 and Mano and Biswas, 2018 as
551 shown recently (Bekturova et al. 2021, Nurbekova et al. 2021). Rosette leaves (250mg) were
552 immersed in 2.5 ml acetonitrile (all acetonitrile mentioned is of HPLC Ultra Gradient Solvent)
553 containing 25 nmol 2-ethylhexanal (as an internal standard) and 0.005% (w/v)
554 butylhydroxytoluene (BHT). The leaves were incubated in a screw-capped glass tube at 60°C
555 for 30 min and the supernatant was collected by decantation. For derivatization of aldehydes,
556 2,4-dinitrophenylhydrazine (DNPH) was purified (recrystallized) as described before (Mano
557 and Biswas, 2018). Briefly, an equal of commercial DNPH was dissolved in 50 ml of warm
558 (60 °C) acetonitrile. Complete dissolved DNPH was chilled gradually (for several hours) and
559 generated crystals were collected through filter paper. DNPH crystals were dissolved in
560 acetonitrile to make 20 mM solution. To derivatize aldehydes with DNPH, 62.5µl of 20mM
561 DNPH (in acetonitrile) and 48.4µl of 99% formic acid (LC-MS quality) were added to the
562 resulting supernatant and incubated at 25°C for 60 min. Thereafter 2.5ml NaCl (5M) and
563 450mg $NaHCO_3$ were added to the mixture for neutralizing formic acid and mixture was
564 shaken at intervals for 10 min. After centrifugation, the upper layer was collected and dried in
565 vacuum and then dissolved in 250 µl acetonitrile. This solution was applied on a Bond Elute
566 C18 cartridge [sorbent mass 200 mg (Agilent Technologies, USA)], which has been pre-
567 washed with 2 ml acetonitrile, and the pass-through (250 µl) and subsequent wash (150 µl
568 acetonitrile) were combined as the eluted solution. Fifteen µl of the eluted solution were
569 analyzed using Thermo Scientific DionexUltiMate 3000 UHPLC system
570 (http://www.dionex.com/en-us/products/liquid-chromatography/lc-systems/lp-87043.html)
571 with Variable Wavelength VWD-3100 detector. The fifteen µl eluted solution was injected into
572 a Wakosil DNPH-II column (4.6 mm x 150 mm(W), No.17193, Wako Pure Chemical
573 Industries, Ltd., Osaka, Japan, http://www.wako-chem.co.jp/english) with the following
574 elution conditions: 1 ml min-1 flow rate, 0–5 min, 100% HPLC quality Eluent A (Wako Pure
575 Chemical Industries) 5–20 min, a linear gradient from 100% A to 100% HPLC quality Eluent

576 B (Wako Pure Chemical Industries); 20–25 min, 100% B, 25–45 min, a linear gradient from
577 100% B to 100% C (acetonitrile). The detection wavelength was 340 nm, and the column
578 temperature was 35°C. Aldehydes were identified by their retention times and the retention
579 times of the detected aldehydes were compared with aldehyde standards in the same run. The
580 content of the aldehydes was calculated from the peak area of the corresponding DNP- carbonyl
581 by using appropriate software [CHROMELEON7 (https://www.thermofisher.com)]. Aldehyde
582 toxicity was examined with 21-day old *aao2* KOs and WT plants as done by us before
583 (Nurbekova at al. 2021). The effect of aldehyde application was photographed as mentioned in
584 the figure legends. ABA concentrations in leaves were determined as previously described
585 (Turečková et al. 2009).
586
587 **Preparation of DNP-aldehyde standards.**
588 DNP-aldehyde standards were prepared as previously described (Mano and Biswass., 2018). 1
589 mM of DNPH (ca. 0.3 g) was dissolved in 20 ml acetonitrile (HPLC Ultra Gradient Solvent).
590 To the dissolved DNPH solution 1 mM of aldehyde and few drops of formic acid were added.
591 The mixture was kept under a chemical hood by stirring. For acetals, such as acrolein, 1 mmol
592 of aldehyde was dissolved in 30 ml of DNPH solution (5 mM in 2 M HCL). After DNP-
593 Aldehyde precipitation, crystals of DNP-aldehyde standards were collected and dried. The mol
594 amount of DNP-derivative is determined by the weight.
595
596 **ACCESSION NUMBERS**
597 Sequence data used in this work can be found in the GenBank/ EMBL data libraries under
598 accession numbers At2g27150 (AAO3), At3g43600 (AAO2), At5g20960 (AAO1).

599 **ACKNOWLEDGMENTS**

600 M.S. thankfully acknowledge a grant from the Israel Center of Research Excellence (Plant
601 Adaptation grant no. 757/12), and M.St. and V.T. thankfully acknowledge a grant from the
602 European Regional Development Fund-Project (No. CZ.02.1.01/0.0/0.0/16_019/0000827).

603

604 **CONFLICT OF INTEREST**

605 All authors have no conflicts of interest to declare.

606

607 **AUTHOR CONTRIBUTIONS**

608 Zh.N. participated in designing the research plans and performed the experiments and analysis;
609 S.S. read and commented on the manuscript; ZD.N. participated in in-gel activity analysis, V.T.
610 and M.St. performed the detection of ABA level; (R.O.)read and commented on the manuscript
611 ; M.S. conceived the original idea, designed the research plan and supervised the research work.
612 The article was jointly written by Zh. N and M.S.

613 **SUPPORTING INFORMATION**

614 The following supplemental materials are available in the online version of this article

615 **Supplemental Figure S1.** Relative transcript expression of AAO2 (At3g43600) and Aldehyde
616 oxidases (AAOs) activity in control and UV-C treated WT, *aao2* [SALK_104895 (KO-95)],
617 *aao1* [At5g20960, SALK_018100, (a1-100)] and *aao3* [At2g27150, SAIL_78_H09 (KO9)]
618 mutant plants**.**

619 **Supplemental Figure S2.** Relative transcript expression of AAO1(At5g20960), AAO2
620 (At3g43600) and AAO3 (At2g27150) in rosette leaves of 23- days post germination
621 *Arabidopsis* WT, *aao1Single (aao1S)* and independent *aao3Singles (aao3S)* mutant plants.

622 **Supplemental Figure S3.** Determination of UV-C-irradiation-induced senescence and
623 senescence-related factors in rosette leaves of *Arabidopsis* wild-type (WT) and AAO1
624 overexpression (AAO1OE) mutant plants.

625 **Supplemental Figure S4**. The effect of exogenously applied benzaldehyde on rosette leaves
626 of wild-type (WT) and *aao2* KO [SALK_104895 (KO-95) and SAIL_563_G09 (KO-563)]
627 mutant plants.

628 **Supplemental Figure S5.** The effect of UV-C irradiation on the transcript expression of *Nine-*
629 *cis-epoxy carotenoid dioxygenase 3 (NCED3-2;* At3g14440*)* gene in rosette leaves of
630 *Arabidopsis* WT and *aao2 KO* [SALK_104895 (KO-95) and SAIL_563_G09 (KO-563)]
631 mutant plants.

632 **Supplemental Figure S6.** The effect of molybdenum cofactor sulfuration and UV-C
633 irradiation on Aldehyde oxidases (AAOs) activity in WT, *aao2* [SALK_104895 (KO-95)] and
634 the molybdenum cofactor sulfurase (*aba3-1,* At1g16540) mutant plants.

635 **Supplemental Figure S7.** The effect of UV-C irradiation or Rose Bengal treatment on the
636 transcript expression of ABA3 (At1g16540) in rosette leaves of *Arabidopsis* WT and *aao2*
637 [SALK_104895 (KO-95) and SAIL_563_G09 (KO-563)] mutant plants.

638 **Supplemental Figure S8.** The effect of UV-C irradiation or Ros Bengal treatment on relative
639 transcript expression of AAO3 (At2g27150) in rosette leaves of *Arabidopsis* WT, *aao2*
640 [SALK_104895 (KO-95) and SAIL_563_G09 (KO-563)] mutant plants.
641
642 **Supplemental Table S1.** Verification of AAO2 (At3g43600) KO mutants (KO-95 and KO-
643 563) homozygosity.
644 **Supplemental Table S2. A.** Details of primers used to carry out quantitative real time PCR
645 analysis and **(B)** results of sequence analysis of the resulting product.
646 **Supplemental Table S3.** Unique peptides of *Arabidopsis* aldehyde oxidases (AAOs)
647 identified by LC-MS.
648

649 **FIGURE LEGENDS**

650 **Figure 1.** Characterization of *Arabidopsis* aldehyde oxidase 2 mutants. **A.** Verification of
651 AAO2 knock out mutants {*aao2* [SALK_104895 (KO-95) and SAIL_563_G09 (KO-563)]}
652 by PCR using the combination of gene specific primers (LP and RP) and specific primer
653 flanking T-DNA insertion stretches (LB 1.3 or LB2, respectively). **B.** Relative transcript
654 expression of *AAO2* (At3g43600) in WT and the two *aao2* mutants' rosette leaves. The
655 expression of the *AAO2* in each genotype was compared against *AAO2* in WT after
656 normalization to *Arabidopsis EF-1a* (At5g60390) as the housekeeping gene product and
657 presented as the relative expression. Values means ± SE (n=3). Differences were compared
658 among all the genotypes and different letters show the significant difference between genotypes
659 (Tukey's honest significant difference, HSD, P value <0.05). **C.** *Arabidopsis* aldehyde oxidases
660 (AAOs) in-gel activity in WT and *aao2* (KO-95 and KO-563). One hundred µg protein extract
661 from three-week old plants' rosette leaves were fractionated by NATIVE PAGE and AO
662 activity detection with 1 mM *trans*-2-hexanal as the substrate was determined in a reaction
663 solution containing 100 mM Tris-HCl (pH 7.5), 1 mM 3-(4,5-dimethylthiazol-2-yl)-2,5-
664 diphenyltetrazolium bromide and 0.1 mM phenazine methosulfate. The arrow indicates the
665 position of the activity bands generated by AAO1 and AAO3 proteins (uppermost band),
666 middle (heterodimer containing AAO2 with AAO1 and/or with AAO3), and AAO2 (lowermost
667 band). Relative intensity (RI) was estimated by using ImageJ software
668 (https://imagej.nih.gov/ij/) for each activity band. The intensity of the upper, middle, and
669 lowest activity bands in WT was used as reference (100%).

670 **Figure 2.** *Arabidopsis* aldehyde oxidases (AAOs) activity assessment in WT and *aao2* [
671 SALK104895 (KO-95)] mutant using different aldehydes as the substrate. One hundred
672 µg protein extracted from rosette leaves of 23-day old WT and KO-95 mutant plants were
673 fractionated by NATIVE PAGE and AO activity with indicated aldehyde as the substrate was
674 carried out. AO enzyme activity was determined in a reaction solution containing 100 mM
675 Tris-HCl (pH 7.5), 1 mM 3-(4,5-dimethylthiazol-2-yl)-2,5-diphenyltetrazolium bromide, 0.1
676 mM phenazine methosulfate and 1 mM aldehydes, except for HNE and abscisic aldehyde that
677 were applied with 0.25 mM and 0.1 mM, respectively. The reaction was stopped after 3h and
678 after 2 h for abscisic aldehyde, by immersing the gel in 5% acetic acid solution. Thereafter gel
679 images were captured and analyzed for relative intensity (RI) using ImageJ software

680 (http://imagej.nih.gov/ij/) for the slowest (uppermost) migrated band intensity compared to the
681 WT uppermost migrated band as reference (100%).

682 **Figure 3.** Determination of UV-C-irradiation-induced senescence and senescence-related
683 factors in rosette leaves of *Arabidopsis* wild-type (WT) and *aao2* KO [SALK_104895 (KO-
684 95) and SAIL_563_G09 (KO-563)] mutant plants. **A.** Representative photograph of WT and
685 *aao2* rosette leaves in response to UV-C irradiation. 21-day post germination plants exposed
686 to 250 mJ of UV-C irradiation were kept in a growth room for 72 hours and thereafter
687 documented. Scale bar=1 cm. Rosette leaves were collected 3 days after UV-C treatment and
688 rosette leaves of plants that were not exposed to UV-C were used as the control. First five
689 leaves, oldest to youngest, from left to right are presented. **B.** Remaining chlorophyll in leaves
690 after UV-C treatment. **C.** Indicated aldehyde profiling in control (blue bars) and UV-C treated
691 (red bars) plants. Leaves from 3 different plants were taken as one replica and the bars show
692 the average of at least 4 replicas. Different letters above the bar indicate significant differences
693 (Tukey-Kramer HSD test, $P<0.05$). Asterisk shows significant differences between treatments
694 within the same genotype (Student's t test, $P < 0.05$). **D.** Aldehyde oxidases (AAOs) in gel
695 activity in control and UV-C treated WT, *aao2* (KO-95), *aao3* [SAIL_78_H09 (KO9)] and
696 *aao1* [SALK_018100 (a1-100)]. 150 µg crude protein extracted from rosette leaves were
697 fractionated by NATIVE PAGE and were used for the in-gel activity, assayed for 1h in solution
698 containing 100 mM Tris-HCl (pH 7.5), 1 mM 3-(4,5-dimethylthiazol-2-yl)-2,5-
699 diphenyltetrazolium bromide, 0.1 mM phenazine methosulfate and 1 mM *trans*-2-nonenal or
700 Benzaldehyde as the aldehyde substrate. The gels were scanned, and intensity of the activity
701 bands was estimated using ImageJ software (http://imagej.nih.gov/ij/) and compared with the
702 intensity obtained with UV-C untreated (control) WT (employed as 100%) and presented as
703 relative intensity (RI).

704 **Figure 4.** Determination of Rose Bengal-induced senescence and senescence-related factors in
705 rosette leaves of *Arabidopsis* wild-type (WT) and *aao2* KO [SALK_104895 (KO-95) and
706 SAIL_563_G09 (KO-563)] mutant plants. **A.** Representative photograph of WT and *aao2*
707 rosette leaves in response to Rose Bengal application. 23 days post germination plants treated
708 with 0.05 mM Rose Bengal were kept in a growth room for 72 hours and thereafter
709 documented. Scale bar=2 cm. First five leaves, oldest to youngest, from left to right are
710 presented. The rosette leaves were collected 17 hours after Rose Bengal treatment and rosette
711 leaves of plants that were not exposed to Rose Bengal were used as the control. **B.** Remaining
712 chlorophyll in first five leaves after Rose Bengal treatment. **C.** Indicated aldehyde profiling in
713 control (blue bars) and Rose Bengal treated (red bars) plants. Leaves from 3 different plants
714 were taken as one replica and the bars show the average of at least 4 replicas. Different letters
715 above the bar indicate significant differences (Tukey-Kramer HSD test, $P<0.05$). Asterisk
716 shows significant differences between treatments within the same genotype (Student's t test, P
717 < 0.05). **D.** Aldehyde oxidases (AAOs) in gel activity in control and Rose Bengal treated WT,
718 *aao2* (KO-95), *aao3* [SAIL_78_H09 (KO9)] and *aao1* [SALK_018100 (a1-100)]. 150 µg
719 crude protein extracted from rosette leaves were fractionated by NATIVE PAGE and were
720 used for the in-gel activity, assayed for 1h in solution containing 100 mM Tris-HCl (pH 7.5),
721 1 mM 3-(4,5-dimethylthiazol-2-yl)-2,5-diphenyltetrazolium bromide, 0.1 mM phenazine
722 methosulfate and 1 mM *trans*-2-nonenal or *trans*-2-Hexanal as the aldehyde substrate. The gels
723 were scanned, and intensity of the activity bands was estimated using ImageJ software
724 (http://imagej.nih.gov/ij/) and compared with the intensity of the activity band obtained with
725 Rose Bengal untreated (control) WT (employed as 100%) and presented as relative intensity
726 (RI).

727 **Figure 5.** Determination of UV-C-irradiation-induced senescence and senescence-related
728 factors in rosette leaves of *Arabidopsis* aldehyde oxidases single mutants *[aao1Single (aao1S)*
729 and *aao3Singles (aao3S)*], *aao2* KO [SALK_104895 (KO-95) and wild-type (WT) plants. **A.**
730 Representative photograph of WT, *aao2, aao1S* and *aao3S1 (aao3S-1, aao3S-12, aao3S-18)*
731 rosette leaves in untreated (control) and UV-C irradiation treated plants. 21-days post
732 germination (DPG) plants exposed to 250 mJ of UV-C irradiation were kept in a growth room
733 for 72 hours and thereafter documented together with rosette leaves of plants not exposed to
734 UV-C (control). Scale bar=2 cm. **B.** The level of remaining chlorophyll in the first seven leaves
735 (oldest to youngest from left to right) after exposing WT and the various mutant plants to UV-
736 C treatment. **C.** Indicated aldehyde profiling in control (blue bars) and UV-C treated (red bars)
737 plants. Leaves from 3 different plants were taken as one replica and the bars show the average
738 of at least 4 replicas. *aao3S* represents the average of the 3 independent *aao3* single mutants.
739 **D.** Aldehyde oxidase 3 (AAO3) in gel activity in control and UV-C treated WT, *aao2* [KO-
740 95), SAIL_563_G09 (KO-563)] and *aao3S (aao3S-1, aao3S-12, aao3S-18)* using abscisic
741 aldehyde as the specific substrate for AAO3. 150 µg crude protein extracted from WT, *aao2*
742 (KO-95 and KO-563) and *aao3S (aao3S-1, aao3S-12, aao3S-18)* rosette leaves were
743 fractionated by NATIVE PAGE and were used for activity. The gels were scanned after 30
744 min, and intensity of the activity bands was estimated using ImageJ software
745 (http://imagej.nih.gov/ij/) and compared with that obtained with UV-C untreated (control) WT
746 (employed as 100%) and presented as relative intensity (RI). **E.** Abscisic acid (ABA) level in
747 rosette leaves of WT, *aao2KO (KO-95, KO-563), aao1S (aao1S-11)* and *aao3S* (*aao3S-1,*
748 *aao3S-12, aao3S-18*) untreated control (blue bars) and UV-C treated (red bars) plants.
749 Different letters above the bar indicate significant difference (Tukey-Kramer HSD test,
750 P<0.05). Asterisk shows significant differences between treatments within the same genotype
751 (Student's t test, P < 0.05).

752 **Figure 6.** Determination of Rose Bengal-induced senescence and senescence-related factors in
753 rosette leaves of *Arabidopsis* aldehyde oxidases single mutants *[aao1Single (aao1S)* and
754 *aao3Singles (aao3S)*], *aao2* KO [SALK_104895 (KO-95) and wild-type (WT) plants. **A.**
755 Representative photograph of WT, *aao2, aao1S* and *aao3S2 (aao3S-7, aao3S-12, aao3S-18)*
756 rosette leaves in untreated (control) and Rose Bengal treated plants. 21-DPG plants treated
757 with 0.05 mM of Rose Bengal were kept in a growth room for 72 hours and thereafter
758 documented. Scale bar=2 cm. **B.** Damage level in leaves as shown in (A) was calculated as
759 described in the materials and methods. Means +-SEM (n = 6). **C.** Indicated aldehyde profiling
760 in control (blue bars) and Rose Bengal treated (red bars) plants. Seventeen hours after Rose
761 Bengal treatment leaves from 3 different untreated (control) or treated plants were taken as one
762 replica and the bars show the average of at least 4 replicas. *aao3S* is average of the 3
763 independent *aao3* singles plants. **D.** Aldehyde oxidases 3 (AAO3) in gel activity in control and
764 Rose Bengal treated WT, *aao2* [KO-95), SAIL_563_G09 (KO-563)] and *aao3S* using abscisic
765 aldehyde as the specific substrate for AAO3. 150 µg crude protein extract from WT, *aao2 (*KO-
766 95, KO-563*)* and *aao3S* rosette leaves was fractionated by NATIVE PAGE and were used for
767 the in-gel activity. The gels were scanned after 1h, and the intensity of the activity bands was
768 estimated using ImageJ software (http://imagej.nih.gov/ij/) and compared with that obtained
769 with Rose Bengal untreated (control) WT (employed as 100%) and presented as relative
770 intensity (RI). **E.** ABA content in rosette leaves of WT, *aao2KO (KO-95, KO-563), aao1S*
771 *(aao1S-11)* and *aao3S* (*aao3S-7, aao3S-12, aao3S-18*) untreated control (blue bars) and Rose
772 Bengal treated (red bars). Different letters above the bar indicate significant differences
773 (Tukey-Kramer HSD test, P<0.05). Asterisk shows significant differences between treatments
774 within the same genotype (Student's t test, P < 0.05).

775

776 **Supplemental Figures**

777 Supplemental **Figure S1**. Relative transcript expression of AAO2 (At3g43600) and Aldehyde
778 oxidases (AAOs) activity in control and UV-C treated WT, *aao2* [SALK_104895 (KO-95)],
779 *aao1* [At5g20960, SALK_018100, (a1-100)] and *aao3* [At2g27150, SAIL_78_H09 (KO9)]
780 mutant plants. A. Transcript expression levels of AAO2 gene in rosette leaves of WT, *aao2*
781 *(*KO-95*), aao1(*a1-100*)* and *aao3* (KO9) 72 hours after UV-C irradiation treatment (red bars)
782 or untreated (blue bars) were compared with the corresponding transcript in WT after
783 normalization to *EF-1a* (At5g60390) transcript as the housekeeping gene and presented as
784 relative expression. Different letters above the bar indicate significant differences (Tukey-
785 Kramer HSD test, P<0.05). Asterisk shows significant differences between treatments within
786 the same genotype (Student's t test, P < 0.05). B. Aldehyde oxidases (AAOs) in gel activity in
787 23 days old WT, *aao1 (*a1-100) and *aao3* (KO9) mutant plants. 150 µg crude protein extract
788 from the rosette leaves of each genotype was fractionated by NATIVE PAGE for the in-gel
789 activity assay in a solution containing 100 mM Tris-HCl (pH 7.5), 1 mM 3-(4,5-
790 dimethylthiazol-2-yl)-2,5-diphenyltetrazolium bromide, 0.1 mM phenazine methosulfate and
791 1 mM acrolein as substrate. The gels were scanned after 2h, and intensity of the activity bands
792 was estimated using ImageJ software (http://imagej.nih.gov/ij/). Each of the obtained
793 intensities was compared with that obtained with UV-C untreated (control) WT (employed as
794 100%) and presented as relative intensity (RI).

795 Supplemental **Figure S2.** Relative transcript expression of AAO1(At5g20960), AAO2
796 (At3g43600) and AAO3 (At2g27150) in rosette leaves of 23- days post germination
797 *Arabidopsis* WT, *aao1Single (aao1S)* and independent *aao3Singles (aao3S)* mutant plants. The
798 expression level of each of the transcripts in WT, *aao1S (aao1S-11) and aao3Ss (aao3S-1,*
799 *aao3S-7, aao3S-11, aao3S-12, aao3S-18)* mutants was compared with the corresponding
800 transcript in WT after normalization to the transcript of *EF-1a (*At5g60390*)*, as the
801 housekeeping gene and presented as relative expression. Different letters above the bar show
802 significant differences (Tukey-Kramer HSD test, P<0.05). *aao1S* was generated by silencing
803 AAO3 in *aao2* [SALK_104895 (KO-95)], and *aao3S* was generated by silencing AAO1 in
804 *aao2(KO-95)* plants or silencing AAO2 in *aao1* [SALK_018100 (a1-100)] plants.

805 Supplemental **Figure S3.** Determination of UV-C-irradiation-induced senescence and
806 senescence-related factors in rosette leaves of *Arabidopsis* wild-type (WT) and AAO1
807 overexpression (AAO1OE) mutant plants. **A.** Representative photograph of WT and AAO1OE
808 rosette leaves in response to UV-C irradiation. 23-day post germination (DPG) plants exposed
809 to 250 mJ UV-C irradiation were kept in the growth room for 72 hours and thereafter
810 documented. Scale bar=1 cm. Rosette leaves were collected 3 days after UV-C treatment and
811 rosette leaves of plants that were not exposed to UV-C were used as the control. The first six
812 leaves, oldest to youngest, from left to right are presented. **B.** Remaining chlorophyll in first
813 six leaves (oldest to youngest from left to right) after UV-C treatment. **C.** Indicated aldehyde
814 profiling in control (blue bars) and UV-C treated (red bars) plants. Leaves from 3 different
815 plants were taken as one replica and the bars show the average of at least 4 replicas. Different
816 letters above the bar indicate significant difference (Tukey-Kramer HSD test, P<0.05). Asterisk
817 shows significant differences between treatments within the same genotype (Student's t test, P
818 < 0.05).

819 Supplemental **Figure S4**. The effect of exogenously applied benzaldehyde on rosette leaves of
820 wild-type (WT) and *aao2* KO [SALK_104895 (KO-95) and SAIL_563_G09 (KO-563)]
821 mutant plants. **A.** The appearance of WT and *aao2KO* rosette leaves 3 days after exogenously
822 applied 4.5 mM benzaldehyde and water applied as the control. The benzaldehyde solution or
823 water (control) were added to the plants grown on plates (23-day post germination (DPG)

plants) for 3 h and thereafter were removed. Arrows indicate damaged area in leaves. Scale bar=1cm. **B.** Remaining chlorophyll detected in the six oldest leaves of benzaldehyde and control treated plants. Different letters above the bars indicate significant differences according to the Tukey-Kramer HSD mean-separation test (P <0.05).

Supplemental **Figure S5.** The effect of UV-C irradiation on the transcript expression of *Nine-cis-epoxy carotenoid dioxygenase 3 (NCED3-2;* At3g14440*)* gene in rosette leaves of *Arabidopsis* WT and *aao2 KO* [SALK_104895 (KO-95) and SAIL_563_G09 (KO-563)] mutant plants. Controls and UV-C treated are marked with blue and red colors respectively. The *NCED3-2* transcript expression in UV-C irradiation treated or control treated WT and *aao2 KO* (KO-95, KO-563) leaves were compared with the respective transcript in WT control after normalization to the *Arabidopsis EF-1a (*At5g60390*)* and presented as the relative expression. Values with different letters above the bar are significantly different according to the Turkey-Kramer HSD mean-separation test (P < 0.05). Asterisk shows significant difference between treatments within the same genotype (Student's t test, P < 0.05).

Supplemental **Figure S6.** The effect of molybdenum cofactor sulfuration and UV-C irradiation on Aldehyde oxidases (AAOs) activity in WT, *aao2* [SALK_104895 (KO-95)] and the molybdenum cofactor sulfurase (*aba3-1,* At1g16540) mutant plants. **A.** AAOs in gel activity of not Sulfurated (NS) and Sulfurated (S) control WT, aao*2* (KO-95) and *aba3* mutant plants using trans-2-nonenal as the substrate. **B.** Aldehyde oxidase 3 in gel activity of NS and S control as well as UV-C treated WT, aao*2* (KO-95) and *aba3* mutant plants with abscisic aldehyde as the specific substrate for AAO3 activity. 150 µg crude protein extracted from UV-C treated or untreated WT, aao*2* (KO-95) and *aba3* rosette leaves that were sulfurated (S) or not sulfurated (NS), was fractionated by NATIVE PAGE for the in-gel activity, assayed for 1h in solution containing 100 mM Tris-HCl (pH 7.5), 1 mM 3-(4,5-dimethylthiazol-2-yl)-2,5-diphenyltetrazolium bromide, 0.1 mM phenazine methosulfate and 1 mM *trans*-2-nonenal or 0.1 mM abscisic aldehyde as the substrate. The gels were scanned, and the intensity of the activity bands was estimated using ImageJ software (http://imagej.nih.gov/ij/) and compared with that obtained with non Sulfurated (NS) WT control (employed as 100%) and presented as relative intensity (RI).

Supplemental **Figure S7.** The effect of UV-C irradiation or Ros Bengal treatment on the transcript expression of ABA3 (At1g16540) in rosette leaves of *Arabidopsis* WT and *aao2* [SALK_104895 (KO-95) and SAIL_563_G09 (KO-563)] mutant plants. **A.** The transcript expression of ABA3 gene in rosette leaves of WT and aao*2* (KO-95, KO-563) 72 hours after UV-C irradiation (red bars) or controls (untreated) (blue bars) were compared with the corresponding transcript in WT after normalization to the transcript of *EF-1a (*At5g60390*)* as the housekeeping gene and presented as relative expression. **B.** The transcript expression of ABA3 (At1g16540) gene in rosette leaves of WT and *aao2* (KO-95, KO-563) 17 hours after Rose Bengal (RB) treated (red bars) or untreated (blue bars) were compared with the corresponding transcript in WT after normalization to the transcript of *EF-1a (*At5g60390*)* as the housekeeping gene and presented as relative expression. Different letters above the bar show significant differences (Tukey-Kramer HSD test, P<0.05). Asterisk shows significant differences between treatments within the same genotype (Student's t test, P < 0.05).

Supplemental **Figure S8.** The effect of UV-C irradiation or Rose Bengal treatment on relative transcript expression of AAO3 (At2g27150) in rosette leaves of *Arabidopsis* WT, *aao2* [SALK_104895 (KO-95) and SAIL_563_G09 (KO-563)] mutant plants. **A.** The transcript expression of AAO3 in rosette leaves of *Arabidopsis* WT, *aao2* (KO-95, KO-563) 72 hours after UV-C irradiation (red bars) or in controls [untreated (blue bars)] were compared with the corresponding transcript in WT after normalization to the transcript of *EF-1a* (At5g60390), as

872 the housekeeping gene and presented as relative expression. **B.** The transcript expression levels
873 of AAO3 gene in rosette leaves KO-95, KO-563 17 hours after Rose Bengal (RB) treated (red
874 bars) or untreated (blue bars) were compared with the corresponding transcript in WT after
875 normalization to the transcript of *EF-1a (*At5g60390*)* as the housekeeping gene and presented
876 as relative expression. Different letters above the bar show significant differences (Tukey-
877 Kramer HSD test, P<0.05). Asterisk shows significant differences between treatments within
878 the same genotype (Student's t test, P < 0.05).

879 **Supplemental Tables**

880 Supplemental **Table S1.** Verification of AAO2 (At3g43600) KO mutants (KO-95 and KO-
881 563) homozygosity. (A) List of primers used for verification of AAO2 KO (SALK_-
882 _104895.22.00.n and SAIL_563_G09) and mutants. (B) *aao2* KO mutants' identity,
883 chromosomes position and amplicons length.

884 Supplemental **Table S2.** (A) Details of primers used to carry out quantitative real time PCR
885 analysis and (B) the results of sequence analysis of the resulting product of AAO2 and aba3.
886 The Sequence of *Arabidopsis Aldehyde oxidase 3 (AAO3; At2g27150), Arabidopsis Aldehyde*
887 *oxidase 1 (AAO1; At5g20960), Nine-cis-epoxy carotenoid dioxygenase 3 (NCED3-2;*
888 *At3g14440)* was already shown in Nurbekova et.al.,2021 and *Elongation factor 1-alpha (EF1α;*
889 *AT5G60390)* was shown in Srivastava et.al., 2017.

890 Supplemental **Table S3.** Unique peptides of *Arabidopsis* aldehyde oxidases (AAOs) identified
891 by LC-MS. In gel activity was conducted as shown in Figure 3D and lower bands from the
892 indicated genotypes were excised followed by their peptide sequencing.

893

894 **REFERENCES**

895 **Akaba S, Leydecker MT, Moureaux T, Oritani T, Koshiba T** (1998) Aldehyde oxidase in
896 wild type and aba1 mutant leaves of Nicotiana plumbaginifolia. Plant Cell Physiol **39**:
897 1281–1286.

898 **Akaba S, Mitsunori S, Dohmae N, Takio K, Sekimoto H, Kamiya Y, Furuya N, Komano**
899 **T, and Koshiba, T.** (1999). Production of homo- and hetero-dimeric isozymes from two
900 aldehyde oxidase genes of Arabidopsis thaliana. J. Biochem **126**: 395–401.

901 **Bekturova A, Oshanova D, Tiwari P, Nurbekova Zh, kurmanbayeva A, Soltabayeva A,**
902 **Yarmolinskyi D, Srivastava S, Tureckova V, Strand A, Sagi M.** (2021). Adenasine 5'
903 phosphosulfate reductase and sulfite oxidase regulate sulfite-induced loss in Arabidopsis.
904 Journal of Experimental Botany **72**: 6447-6466.

905 **Biswas MS, Mano J** (2016) Reactive carbonyl species activate caspase-3-like protease to
906 initiate programmed cell death in plants. Plant Cell Physiol **57**: 1432–1442.

907 Bittner F, Oreb M, Mendel RR. (2021) ABA3 is a molybdenum cofactor sulfurase required
908 for activation of aldehyde oxidase and xanthine dehydrogenase in Arabidopsis thaliana. J
909 Biol Chem 276: 40381–40384.

910 **Bottcher C, Chapman A, Fellermeier F, Choudhary M, Scheel D, Glawischnig E** (2014)
911 The biosynthetic pathway of indole-3-carbaldehyde and indole-3-carboxylic acid
912 derivatives in Arabidopsis. Plant Physiol **165**: 841–853.

913 **Bradford, M.M.,** (1976). A rapid and sensitive method for the quantitation of microgram
914 quantities of protein utilizing the principle of protein-dye binding. Anal Biochem **72**: 248–
915 254.

916 **Brychkova G, Alikulov Z, Fluhr R, Sagi M** (2008) A critical role for ureides in dark and
917 senescence-induced purine remobilization is unmasked in the Atxdh1 Arabidopsis
918 mutant. Plant J **54**: 496–509.

919 **Brychkova G, Xia Z, Yang G, Yesbergenova Z, Zhang Z, Davydov O, Fluhr R, Sagi M**
920 (2007) Sulfite oxidase protects plants against sulfur dioxide toxicity. Plant J **50**: 696–
921 709.

922 **Clough S J, Bent A F(1998)** Floral dip: a simplified method for agrobacterium-mediated
923 transformation of Arabidopsis thaliana. Plant J **6**: 735-743.

924 **Havaux M, Triantaphylide C** (2009) Singlet oxygen in plants : production , detoxification
925 and signaling. Trends in Plant Science. **14**: 219–228.

926 **Ibdah M, Chen YT, Wilkerson CG, Pichersky E** (2009) An aldehyde oxidase in
927 developing seeds of arabidopsis converts benzaldehyde to benzoic acid. Plant Physiol
928 **150**: 416–423.

929 **Knox JP, Dodge AD** (1984) Photodynamic damage to plant leaf tissue by rose bengal. Plant
930 Science Letters 37: 3-7.

931 **Koshiba T, Saito E, Ono N, Yamamoto N, Sato M** (1996) Purification and Properties of
932 Flavin- and Molybdenum-Containing Aldehyde Oxidase from Coleoptiles of Maize.
933 Plant Physiol **110**: 781–789.

934 **Koiwai H, Nakaminami K, Seo M, Mitsuhashi W, Toyomasu T, and Koshiba T** (2004)
935 Tissue-Specific Localization of an Abscisic Acid, Enzyme AAO3, in Arabidopsis**.** Plant
936 Physiol **134**: 1697–1707.

937 **Kurmanbayeva A, Bekturova A, Srivastava S, Soltabayeva A, Asatryan A, Ventura Y,**
938 **Khan MS, Salazar O, Fedoroff N and Sagi M** (2017) Higher novel L-Cys degradation
939 activity results in lower organic-S and biomass in sarcocornia than the related Saltwort,
940 Salicornia. Plant Physiol **175**: 272–289.

941 **Laemmli, U.K** (1970). Cleavage of structural proteins during the assembly of the head of
942 bacteriophage T4. Nature **227**: 680-685.

943 **Mano J, Tokushige K, Mizoguchi H, Fujii H, and Khorobrykh S.** (2010). Accumulation of
944 lipid peroxide-derived, toxic α,β-unsaturated aldehydes (E)-2-pentenal, acrolein and (E)-
945 2-hexenal in leaves under photoinhibitory illumination. Plant Biotechnol **27**: 193–19.

946 **Mano J, Kanameda S, Kuramitsu R, Matsuura N, Yamauchi Y** (2019) Detoxification of
947 reactive carbonyl species by glutathione transferase tau isozymes. Front Plant Sci **10**: 1–
948 7.

949 **Mano J, Nagata M, Okamura S, Shiraya T, Mitsui T** (2014) Identification of oxidatively
950 modified proteins in salt-stressed arabidopsis: A carbonyl-targeted proteomics approach.
951 Plant Cell Physiol **55**: 1233–1244.

952 **Mano J, Torii Y, Hayashi S ichiro, Takimoto K, Matsui K, Nakamura K, Inzé D,**
953 **Babiychuk E, Kushnir S, Asada K** (2002) The NADPH:Quinone oxidoreductase P1-ζ-
954 crystallin in Arabidopsis catalyzes the α,β-hydrogenation of 2-alkenals: Detoxication of
955 the lipid peroxide-derived reactive aldehydes. Plant Cell Physiol **43**: 1445–1455.

956 **Mano J and Biswas M.S.** (2018) Analysis of reactive carbonyl species generated under
957 oxidative stress. Methods Mol Biol **1742**: 117-124.

958 **Matsui K, Sugimoto K, Kakumyan P, Khorobrykh S, Mano J.** (2009) Volatile oxylipins
959 formed under stress in plants. Methods Mol Biol **580**: 17-27.

960 Mendel RR. (2022) The History of the Molybdenum Cofactor—A Personal View. Molecules
961 27, 4934.

962 **Nurbekova Z, Srivastava S, Standing D, Kurmanbayeva A, Bekturova A, Soltabayeva A,**
963 **Oshanova D, Turečková V, Strand M, Biswas MS, Mano J and Moshe S** (2021)
964 Arabidopsis aldehyde oxidase 3, known to oxidize abscisic aldehyde to abscisic acid,
965 protects leaves from aldehyde toxicity. Plant J **108**: 1439–1455.

966 **Oberschall A, Deák M, Török K, Sass L, Vass I, Kovács I, Fehér A, Dudits D and**
967 **Horváth G V.** (2000) A novel aldose/aldehyde reductase protects transgenic plants
968 against lipid peroxidation under chemical and drought stresses. Plant J **24**: 437–446.

969 **Omarov RT, Akaba S, Koshiba T, Lips SH** (1999) Aldehyde oxidase in roots, leaves and
970 seeds of barley (Hordeum vulgare L.). J Exp Bot **50**: 63–69.

971 **Omarov RT, Sagi M, Lips SH** (1998) Regulation of aldehyde oxidase and nitrate reductase
972 in roots of barley (Hordeum vulgare L.) by nitrogen source and salinity. J Exp Bot **49**:
973 897–902.

974 **Oshanova D, Kurmanbayeva A, Bekturova A, Soltabayeva A, Nurbekova Zh, Standing**
975 **S, Dubey A K and Sagi M** (2021) level of sulfite oxidase activity affects sulfur and
976 carbon metabolism in Arabidopsis. Frontier in Plant Science **12,** p690830.

977 **Rothe GM** (1974). Aldehyde oxidase isoenzymes (E.C.1.2.3.1) in potato tubers (Solanum
978 tuberosum). Plant Cell Physiology.**15**: 493–499.

979 **Ruggiero B, Koiwa H, Manabe Y, Quist TM, Inan G, Saccardo F, Joly RJ, Hasegawa**
980 **PM, Bressan RA, Maggio A** (2004) Uncoupling the Effects of Abscisic Acid on Plant
981 Growth and Water Relations . Analysis of sto1 / nced3 , an Abscisic Acid-Deficient but
982 Salt Stress-Tolerant Mutant in Arabidopsis. **136**: 3134–3147.

983 **Sagi M, Fluhr R, Lips SH** (1999) Aldehyde oxidase and xanthine dehydrogenase in a flacca
984 tomato mutant with deficient abscisic acid and wilty phenotype Plant Physiol **120**: 571-
985 577.

986 **Sagi M, Omarov RT, Lips SH** (1998) The Mo-hydroxylases xanthine dehydrogenase and
987 aldehyde oxidase in ryegrass as affected by nitrogen and salinity. Plant Sci **135**: 125–
988 135.

989 **Sagi M, Scazzocchio C, Fluhr R** (2002) The absence of molybdenum cofactor sulfuration is
990 the primary cause of the flacca phenotype in tomato plants. Plant J **31**: 305–317.

991 **Seo M, Koiwai H, Akaba S, Komano T, Oritani T, Kamiya Y, Koshiba T** (2000a)
992 Abscisic aldehyde oxidase in leaves of Arabidopsis thaliana. Plant J **23**: 481–488.

993 **Seo M, Peeters AJM, Koiwai H, Oritani T, Marion-Poll A, Zeevaart JAD, Koornneef M,**
994 **Kamiya Y, Koshiba T** (2000b) The Arabidopsis aldehyde oxidase 3 (AAO3) gene
995 product catalyzes the final step in abscisic acid biosynthesis in leaves. Proc Natl Acad
996 Sci **97**: 12908–12913.

997 **Seo M. and Koshiba T.** (2002). Complex regulation of ABA biosynthesis in plants. Trends
998 Plant Sci **7**: 41–48.

999 **Srivastava S, Brychkova G, Yarmolinsky D, Soltabayeva A, Samani T, Sagi M** (2017)
1000 Aldehyde Oxidase 4 Plays a Critical Role in Delaying Silique Senescence by Catalyzing
1001 Aldehyde Detoxification. Plant Physiol **173**: 1977–1997.

1002 **Stiti N, Adewale IO, Petersen J, Bartels D, Kirch HH** (2011) Engineering the nucleotide
1003 coenzyme specificity and sulfhydryl redox sensitivity of two stress-responsive aldehyde
1004 dehydrogenase isoenzymes of Arabidopsis thaliana. Biochem J **434**: 459–471.

1005 **Sunkar R, Bartels D, Kirch HH** (2003) Overexpression of a stress-inducible aldehyde
1006 dehydrogenase gene from Arabidopsis thaliana in transgenic plants improves stress
1007 tolerance. Plant J **35**: 452–464.

1008 **Sussmilch FC, Brodribb T J, McAdam AMS** (2017)Up-regulation of NCED3 and ABA
1009 biosynthesis occur within minutes of a decrease in leaf turgor but AHK1 is not required.
1010 J Exp Bot **68:** 2913-2918.

1011 **Triantaphylides C, Krischke M, Hoeberichts FA, Ksas B, Gresser G, Havaux M,**
1012 **Breusegem F Van, Mueller MJ** (2008) Singlet Oxygen Is the Major Reactive Oxygen
1013 Species Involved in Photooxidative Damage to Plants. Plant Physiol **148**: 960–968.

1014 **Widhalm JR, Dudareva N** (2015) A familiar ring to it: Biosynthesis of plant benzoic acids.
1015 Mol Plant **8**: 83–97.

1016 **Yamauchi Y, Furutera A, Seki K, Toyoda Y, Tanaka K, Sugimoto Y** (2008)
1017 Malondialdehyde generated from peroxidized linolenic acid causes protein modification
1018 in heat-stressed plants. Plant Physiol Biochem **46**: 786–793.

1019 **Yamauchi Y, Hasegawa A, Taninaka A, Mizutani M, Sugimoto Y** (2011) NADPH-
1020 dependent reductases involved in the detoxification of reactive carbonyls in plants. J
1021 Biol Chem **286**: 6999–7009.

1022 **Yergaliyev TM, Nurbekova Z, Mukiyanova G, Akbassova A, Sutula M, Zhangazin S,**
1023 **Bari A, Tleukulova Z, Shamekova M, Masalimov ZK, Omarov R** (2016) The
1024 involvement of ROS producing aldehyde oxidase in plant response to Tombusvirus
1025 infection. Plant Physiol Biochem **109**: 36–44.

1026 **Yesbergenova Z, Yang G, Oron E, Soffer D, Fluhr R and Sagi M.** (2005). The plant Mo-
1027 hydroxylases aldehyde oxidase and xanthine dehydrogenase have distinct reactive
1028 oxygen species signatures and are induced by drought and abscisic acid. Plant J **42**: 862–
1029 876.

1030 **Zdunek-Zastocka E, Omarov RT, Koshiba T, Lips HS** (2004) Activity and protein level
1031 of AO isoforms in pea plants (Pisum sativum L.) during vegetative development and in
1032 response to stress conditions. J Exp Bot **55**: 1361–1369.

1033

1034